Adaptive emission reduction approach to reach any global warming target

Jens Terhaar, Thomas L. Frölicher, Mathias T. Aschwanden, Pierre Friedlingstein, Fortunat Joos

Adaptive emission reduction approach to reach any global warming target

Jens Terhaar[1,2*], Thomas L. Frölicher[1,2], Mathias T. Aschwanden[1,2], Pierre Friedlingstein[3,4], Fortunat Joos[1,2]

[1] Climate and Environmental Physics, Physics Institute, University of Bern, Switzerland

[2] Oeschger Centre for Climate Change Research, University of Bern, Switzerland

[3] College of Engineering, Mathematics and Physical Sciences, University of Exeter, Exeter EX4 4QF, UK

[4] Laboratoire de Météorologie Dynamique, Institut Pierre-Simon Laplace, CNRS-ENS-UPMC-X, Paris, France

***Jens Terhaar**

Climate and Environmental Physics, Physics Institute

University of Bern

Sidlerstrasse 5

3012 Bern

Switzerland

jens.terhaar@unibe.ch

The parties of the Paris Agreement agreed to keep global warming well below 2°C and pursue efforts to limit it to 1.5°C. A global stocktake is instituted to assess the necessary emissions reductions every five years. Here, we propose an adaptive approach to quantify successively global emissions reductions that allow reaching a temperature target within ±0.2°C – solely based on regularly updated observations of past temperatures, radiative forcing, and emissions statistics and not on climate model projections. Testing this approach using an Earth System Model of Intermediate Complexity demonstrates that defined targets can be reached following a smooth emissions pathway. The adaptive nature makes the approach robust against inherent uncertainties in observational records, climate sensitivity, effectiveness of emissions reduction implementations, and the metric to estimate CO_2 equivalent emissions. This approach allows developing emission trajectories for CO_2, CH_4, N_2O, and other agents that iteratively adapt to meet a chosen temperature target.

Human-made emissions of greenhouse gases (GHG) and other radiative forcing agents have led to global warming of around 1.2°C by 2020[1] with already observable negative impacts on the world's climate and ecosystems[2,3]. To limit the impact from further warming[4,5], 191 countries signed the Paris agreement to "keep global warming well below 2°C and to pursue efforts to limit it to 1.5°C" by reducing GHG emissions[6]. As a central part of the agreement, a regular five-year stocktake process was instituted to assess collective progress in reducing emissions over the previous five-year period and to reassess the necessary global emission reductions for the following five years and beyond. Each signatory country provides its nationally determined contributions (NDCs) to the globally necessary GHG emissions reductions.

These necessary reductions to reach a chosen temperature target are often derived using the concept of a remaining emissions budget (REB)[2,7–9]. Such a REB quantifies the total allowed emissions that can still be emitted from the present-day onwards before a temperature target is reached. In the past, REBs usually only included CO_2[8–12]. Non-CO_2 forcing agents were generally included as prescribed, scenario-dependent, climate forcing, bringing an additional uncertainty into the remaining carbon budget[8–13]. To consider emissions of different radiative forcing agents and precursors in one budget, the concepts of Global Warming Potential (GWP)[14] and CO_2-forcing equivalent (CO_2-fe) emissions[7,15,16] can be used. The GWP for a time horizon of 100 years (GWP-100) is the metric applied by the parties of the Paris Agreement, although GWP-100 equivalent emissions from different gases do not result in identical forcing trajectories and climate impacts[7,15,17–19] and other metrics can be additionally used for reporting[20]. CO_2-fe emissions are defined as the amount of CO_2 emissions that would cause the same radiative forcing trajectory as emissions from a non-CO_2 agent (e.g., methane). Thus, the CO_2-fe metric is best suited to compare emissions from different agents in the context of forcing and temperature stabilization pathways. However, even when non-CO_2 emissions are transferred to CO_2-fe emissions and added to the total REB

and not treated as an additional uncertainty of the remaining carbon emissions budget, estimations of the REB in 2020 that allows reaching the 1.5°C temperature target still *likely* vary by a factor of more than two (130–300 Pg C)[7,21].

This range mainly stems from uncertainties in the global temperature response to changes in radiative forcing agents and precursors[8,22–25], historical CO_2-fe emissions[7], historical anthropogenic warming[26–29], change in temperatures after net zero CO_2-fe emissions are reached[30], and future sources and sinks of CO_2 and other agents[30–36]. Furthermore, natural interannual-to-decadal variability in temperature[37–39], and land and ocean carbon and heat sinks[33,40] may mask effects of GHG emissions reductions[41,42].

The large REB uncertainties may hamper efforts to establish ambitious NDCs and could potentially lead to insufficient global emission reductions, large global warming, and severe consequences for natural and human systems[2,43,44]. Therefore, emissions reductions should be estimated at each stocktake using approaches that side-step these uncertainties and allows smoothly approaching a temperature target. Such approaches should be transparent, verifiable, and, to the extent possible, objective to foster their acceptance as well as the implementation of the implied near-term emissions reduction measures. Such a science-based approach to guide near-term emission reduction policies is currently missing.

The Adaptive Emissions Reduction Approach (AERA)

Here, we propose an Adaptive Emissions Reduction Approach (AERA) to estimate the necessary emission reductions until temperature stabilization successively every five years (e.g., 2025, 2030, …) as foreseen by the stocktake mechanism. By adapting emissions every five years, the AERA works like a control system that corrects emissions based on the realized warming to eventually approach a prescribed temperature

target within a narrow range (±0.2°C). For example, a temperature target of 1.75°C may be chosen to estimate the emissions for keeping "global warming well below 2°C". At a future stocktake, the temperature target can be re-defined, for example "to pursue efforts to limit it to 1.5°C".

The AERA only relies on global surface temperature observations, radiative forcing (RF), and emissions data, and does not rely on any Earth system model projections. Its adaptive nature ensures that emission reductions are quantified that allow meeting the foreseen temperature target, irrespective of uncertainties in understanding the climate system. Such adaptive learning and stepwise adjustment of the emission reduction target has been shown to help reducing costs[45] and to avoid strong negative outcomes for the economy and the environment[44].

The AERA consists of three main steps: (1) determining the past anthropogenic warming and hence the remaining warming allowed, (2) estimating the remaining CO_2-fe emission budget, and (3) proposing a future CO_2-fe emission curve until temperature stabilization (Figure 1; see Methods). First, the anthropogenic warming is calculated from observed global mean surface temperature (GMST) time-series using the past RF of all relevant forcing agents (labelled as 'Step 1' in Figure 1)[46]. This approach removes temperature changes from natural variability and non-anthropogenic forcing, such as volcanic eruptions and changes in solar activity, by fitting an Impulse-Response Function[47,48] to the RF and GMST time-series, only leaving the anthropogenic contribution to the observed warming. Alternatively, natural, interannual-to-decadal variability in GMST may also be removed by applying a smoothing spline or another low pass filter[49,50]. Once the realized anthropogenic warming is determined, the remaining warming between the temperature target and the realized anthropogenic warming is estimated by difference.

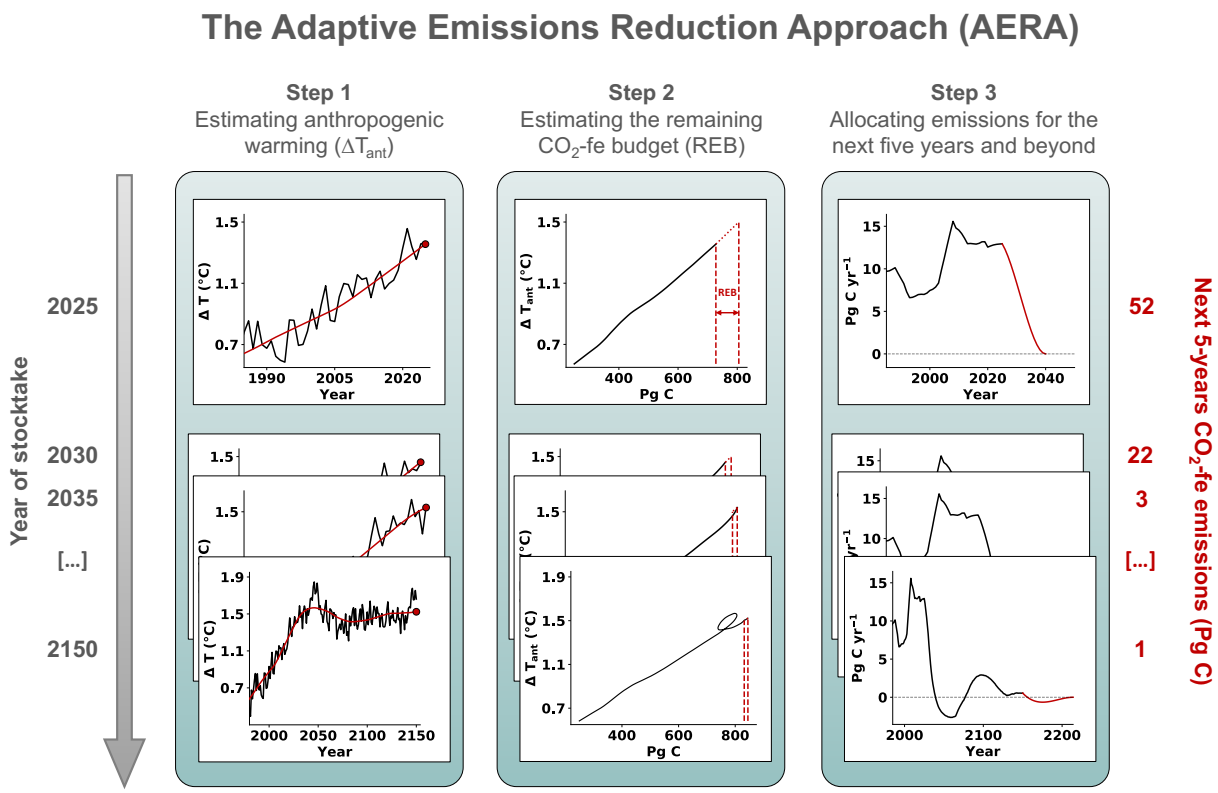

Fig. 1. Schematic of the Adaptive Emission Reduction Approach to limit global warming. The three steps are repeated at the year of each stocktake (indicated on the left) to determine allowable emissions for the next five-year period (red numbers on the right) from temperature observations and forcing and emissions statistics. The approach is illustrated using results from one Bern3D-LPX simulation with ECS=3.2°C as a surrogate for future observations (black lines in insets). Step 1: Estimation of the anthropogenic warming (red lines in inset) at the time of the stocktake from past time-series of GMST (black line) and anthropogenic radiative forcing. Step 2: Estimation of the remaining CO_2-fe emissions budget (REB; space between dashed red lines) based on the observed linear relationship between anthropogenic warming (ΔT_{ant}) and cumulative CO_2-fe emissions (black line). Step 3: Allocation of the REB over the next five years and beyond using a cubic function with minimal slope changes (red line). The approach stabilizes ΔT_{ant} close to the given target, here 1.5°C, as illustrated in the bottom left inset.

Second, the REB of CO_2-fe emissions is estimated using the transient climate response to cumulative emissions (TCRE)[51,52] , determined as the ratio of past warming and past cumulative CO_2-fe emissions (Step 2 in Figure 1). Mathematically, the REB is estimated as the remaining warming until the temperature target divided by TCRE. Therefore, we rely here on the near-linear relationship between cumulative CO_2-fe emission and warming over the past and the assumption that this relationship holds for the near-future[14,53].

When quantified, the REB of CO_2-fe emissions is distributed over the future years (Step 3 in Figure 1). Many possible future CO_2-fe emission curves may exist for one specific REB with different lengths and economic and political assumptions[54]. For simplicity, we use a cubic polynomial function and chose the parameters of the cubic function and its length, i.e., the time until the REB is exhausted, by minimizing the curvature. Thereby, we assume that smaller changes in the trend of CO_2-fe emission curves are easier to implement. It may happen that the curve with the smallest curvature has positive emissions that are later compensated by negative emissions, which would result in a temporary temperature overshoot that could be harmful to the economy[55,56] and ecosystems[57,58]. To reduce the risk of such an overshoot, we also minimized exceedance emissions, i.e., negative emissions if the REB is still positive or positive emissions if the REB is negative. A negative REB can occur if the anthropogenic warming or the TCRE turns out to be larger than estimated in the previous stocktakes.

The three steps of the AERA are intended to be repeated every five years at each stocktake (Figure 1). At each stocktake, the determined future CO_2-fe emission curve until temperature stabilization can be split into contributions from CO_2, CH_4, and N_2O emissions, as well as contributions from other non-CO_2 forcing agents. This split may be achieved using a metric of choice, for example CO_2-fe emissions, which captures the temperature change per CO_2-fe emissions precisely[7,15–17] or GWP-100[18,19,59], which is simpler and can

nevertheless lead to relatively good results in terms of mitigation costs and climate outcomes[60,61]. Independent of the metric to split the CO_2-fe emissions into CO_2 and non-CO_2 emissions, the AERA adjusts the future CO_2-fe emission curve every five years based on the most up-to-date observations of GMST, RF, and CO_2-fe emissions. If the anthropogenic warming will turn out to be larger or smaller than anticipated by the time of the next stocktake, the adaptive nature of the AERA will adjust this successively, much like a control system with a feedback loop. These regular adaptations successively correct for inherent uncertainties of the respective system, here the estimation of the realized anthropogenic warming and the response of GMST to anthropogenic emissions.

Testing the AERA with an Earth System Model

Uncertainties are not explicitly considered in a control system, c.f., the AERA, but they determine how well the control system is functioning. We demonstrate that the AERA allows to reach a chosen temperature level, also those well below 2°C, within the uncertainty with which the anthropogenic warming can be determined (±0.2°C)[26–29], independent of uncertainties in the Earth's temperature sensitivity to GHGs and other agents, the strength of the land and ocean carbon sinks, radiative forcing estimates, the split-up of CO_2-fe emissions in CO_2, CH_4, and N_2O emissions and the applied method (CO_2-fe or GWP-100), and under deviations between emission reductions quantified by the AERA versus those implemented. To that end, we used the Earth System Model of Intermediate Complexity Bern3D-LPX[62,63] under nine different configurations with varying atmospheric sensitivity to atmospheric forcing agents and varying ocean mixing (see methods). These configurations cover the range of estimates of the transient climate response (1.3-2.5°C)[24] and equilibrium climate sensitivities (1.9-5.7°C)[24] (see Methods). Depending on the configuration, the simulated anthropogenic warming in 2020 with prescribed historical CO_2 emissions and non-CO_2 radiative forcing ranges from 0.64 to 1.48°C versus 1.23±0.20°C from

observations (Extended Data Figure 1). The remaining warming in the ensemble would deviate from the observational estimate when prescribing a fixed target in the model. To address the uncertainty in remaining emissions, the remaining warming in 2020 is set to the observational estimate (0.27°C for the 1.5°C target, see Methods) regardless of their simulated warming up to 2020.

Here, we tested the AERA for two fixed temperature targets (1.5°C and 2.0°C) and for a peak and decline case with a temperature target of 1.75°C until 2050 to "keep global warming well below 2°C", but from 2050 onwards, the target is reduced at each stocktake by 0.025°C and reaches 1.5°C in 2100 "to pursue efforts to limit it to 1.5°C"[6]. The target could be further reduced to avoid any exceedance of the 1.5°C limit. The choice to which extent emissions are reduced by reducing CO_2 emissions versus reducing emissions of any other agents are not dictated by the AERA. We exemplify trade-offs in emissions by exploring different choices, e.g., regarding GHG and aerosol emissions reductions. In the standard simulation, CO_2, CH_4, and N_2O emission curves evolve proportional in time after 2025 (Figure 2d-f). An updated reduced form chemistry model[64] is used to calculate non-CO_2 GHG and aerosol radiative forcing from emissions (see Methods). Eventually, the emission curves for individual agents are chosen for which the resulting CO_2-fe emissions from all forcing agents match best the CO_2-fe emissions from the AERA. Atmospheric CO_2 and GMST for the next five-year period are then simulated by the Bern3D-LPX model using the AERA-estimated CO_2 fossil fuel emissions, non-CO_2 forcing, and CO_2 emissions from land use change.

The simulations demonstrate that the AERA allows reaching a chosen temperature level almost exactly at the end of the 22nd century and already within the uncertainty to which anthropogenic warming can be determined (±0.2°C)[26–29] in the second half of the 21st century independent of the model's configuration (Figure 2a). A temporal, small overshoot may occur if the REB was initially overestimated.

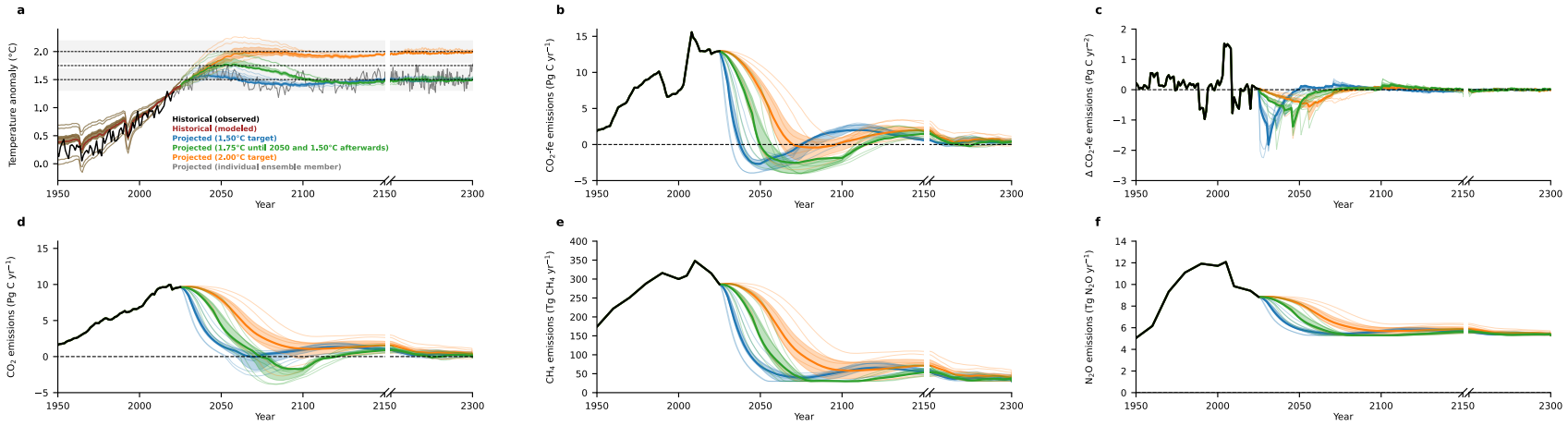

Fig. 2. Globally averaged surface atmospheric temperature anomaly with respect to 1850-1900, CO_2-fe emissions, their annual rate of change, as well as CO_2, CH_4, and N_2O emissions following the adaptive emission reduction approach. (a) Temperature anomalies with respect to 1850-1900, **(b)** CO_2-fe emissions, and **(c)** their annual rate of change if the AERA is applied every five years starting in the year 2025 for the 1.5°C target (blue) and the 2.0°C target (orange), as well as the AERA-calculated emission curves for the proportionally evolving **(d)** CO_2, **(e)** CH_4, and **(f)** N_2O are shown. CH_4, and N_2O emissions cannot descend below the thresholds 30 Tg CH_4 yr^{-1} and 5.3 Tg N_2O yr^{-1}, respectively, due to the difficulty in abating CH_4 and N_2O emissions from agricultural and livestock sectors (see Methods for the choice of these thresholds). Temperature and emission curves are also shown if the AERA is applied with a temperature target of 1.75°C until 2050 and from 2050 onwards this target is stepwise reduced at each stocktake to 1.5°C in 2100 (green). The thick solid lines show the average of the 8 simulations with varying magnitude and timing of added inter-annual temperature variability of the Bern3D-LPX model configuration with an ECS of 3.2°C, the thin solid lines show the same for the remaining 8 configurations covering ECS from 1.9 to 5.7°C, and the shaded area shows the range of all configurations that fall within the likely range of ECS as defined by Sherwood et al. (2020)[24]. The grey shading in **(a)** indicates the uncertainty with which the anthropogenic warming can be determined (±0.2°C)[26–29] for the 1.5°C and 2.0°C targets.

For the fixed 1.5°C target case, the resulting CO_2-fe emissions curves descend quickly (blue lines in Figure 2b), reach zero CO_2-fe emissions by 2038 (2033-2048, the central estimate is the mean over 8 simulations with different superimposed interannual variability (see methods) from the ECS=3.2 model configuration, and the range is the spread of the ensemble means across the remaining 8 model configurations with ECS varying from 1.9°C to 5.7°C), become negative afterward, peak at -2.7 (-4.0 to -1.6) Pg C yr^{-1}, and eventually converge to zero emissions after 2150. If CH_4 and N_2O emissions decrease strongly (Figures 2e,f), net negative CO_2 emissions are not necessary to limit warming to 1.5°C, but CO_2 emissions still approach zero emissions (Figure 2d).

For the fixed 2.0°C target, the resulting CO_2-fe emissions curves (orange lines in Figure 2b) descend less rapidly, reach zero emissions by 2070 (2050-after 2300), and peak at negative emissions of -0.4 (-3.5 to +1.0) Pg C yr^{-1}. The cumulative CO_2 equivalent emissions for the 2°C target, using GWP-100, are 310 Pg C until 2050 and 543 Pg C until 2100, estimated from the AERA-derived CO_2, CH_4, and N_2O emissions. These CO_2 equivalent emissions are similar to estimates by the Climate Action Tracker[65] when assuming that all national pledges and targets are implemented (313 Pg C in 2050 and 513 Pg C in 2100), confirming that stabilizing warming at 2.0°C is possible in this optimistic scenario[66]. Maximum annual CO_2-fe emission reductions for the 2.0°C target are considerably smaller than the necessary reductions for the 1.5°C target (Figure 2c). Furthermore, the timing when zero CO_2-fe emissions need to be reached are in line with previous estimates based on the time of the peak of radiative forcing[67].

The peak and decline case demonstrates that the AERA can also be applied with a temperature target that changes over time (green lines in Figure 2). In the case where the temperature target is reduced from 1.75°C in 2050 to 1.50°C in 2100, the 2°C warming is never exceeded. Negative CO_2-fe emissions are needed until the beginning of the 22nd century. These negative CO_2-fe emissions are realized by negative

225 CO_2 emissions because CH_4 and N_2O emissions have already reached their assumed minima due to the
226 difficulty in abating CH_4 and N_2O emissions from agricultural and livestock sectors (see Methods). This
227 peak and decline simulation shows that net-zero emissions in the second half of the 21st century (Article
228 4.1 of the Paris Agreement[6]) would be sufficient to "keep global warming well below 2°C, if strong
229 emission reductions were implemented in the first half of the 21st century.
230
231 The relative smoothness of the emission curves (Figure 2b, d-f) demonstrates that the projected CO_2-fe
232 emission curves as well as the associated CO_2, CH_4 and N_2O emissions curves by the AERA will need only
233 relatively small adjustments every five years. Therefore, the longer-term projections of CO_2-fe emission
234 curves were reliable and less frequent adjustments may be sufficient. Even if CO_2-fe emission curves were
235 adjusted by the AERA only every 10 years, the resulting CO_2-fe emission curves look almost identical
236 (Extended Data Figure 2). However, small changes at every stocktake are still unavoidable as the REB
237 remains uncertain. The initial REB guess can be different from the final emissions budget because the
238 linearity between warming and cumulative emissions does not hold strictly in all configurations when
239 emissions approach zero, partly due to unrealized warming (or cooling) from past CO_2-fe emission (i.e.,
240 the zero-emission commitment[30]) that varies between model configurations. For Bern3D-LPX,
241 temperatures decrease slightly in the decades after zero emissions are reached[30]. This decrease is
242 automatically corrected by the AERA by slightly increasing CO_2-fe emissions. Despite these uncertainties
243 in the initial estimate of the REB, the adaptive nature of the AERA allows reaching the temperature target
244 while keeping changes in the CO_2-fe emission curve as small as possible.
245
246 Furthermore, we tested the robustness of the AERA under varying pathways of CH_4 and N_2O emission
247 curves and aerosol radiative forcing, by performing three more simulations for the 1.5°C target (Figure 3
248 - violet, red, and ochre curves). Independent of the prescribed non-CO_2 emissions and radiative agents,

249 the respective CO_2-fe emission curves remain almost indistinguishable and temperature stabilization is
250 reached by the AERA in each case (Extended Data Figure 3). However, the necessary CO_2 emission
251 reductions (Figure 3a) depend strongly on the corresponding reduction in CH_4 and N_2O emissions and
252 aerosol radiative forcing. When the magnitude of the aerosol forcing decreases faster (violet curves),
253 slightly stronger reductions in CO_2, CH_4, and N_2O emissions are needed. In an idealized 'solar radiation
254 management' case where aerosols are artificially emitted in the atmosphere after 2025 (red curves), CO_2,
255 CH_4, and N_2O emissions reductions would only need to start 10-15 years later than in the standard case
256 (blue curves), while the necessary reduction rates of CO_2, CH_4, and N_2O emissions would remain similar.
257 Moreover, once the solar radiation management would stop (not simulated here), strong reductions in
258 CO_2, CH_4, and N_2O emissions would be necessary immediately[68,69]. In the extreme case, where only
259 emissions from non-CO_2 gases may be reduced but CO_2 remains constant, temperature cannot be
260 stabilized (Extended Data Figure 4). Although reductions of non-CO_2 emissions can compensate for
261 reductions in CO_2 emissions for some decades, continuing CO_2 emissions will lead to further increases
262 atmospheric CO_2 and hence the global temperature.

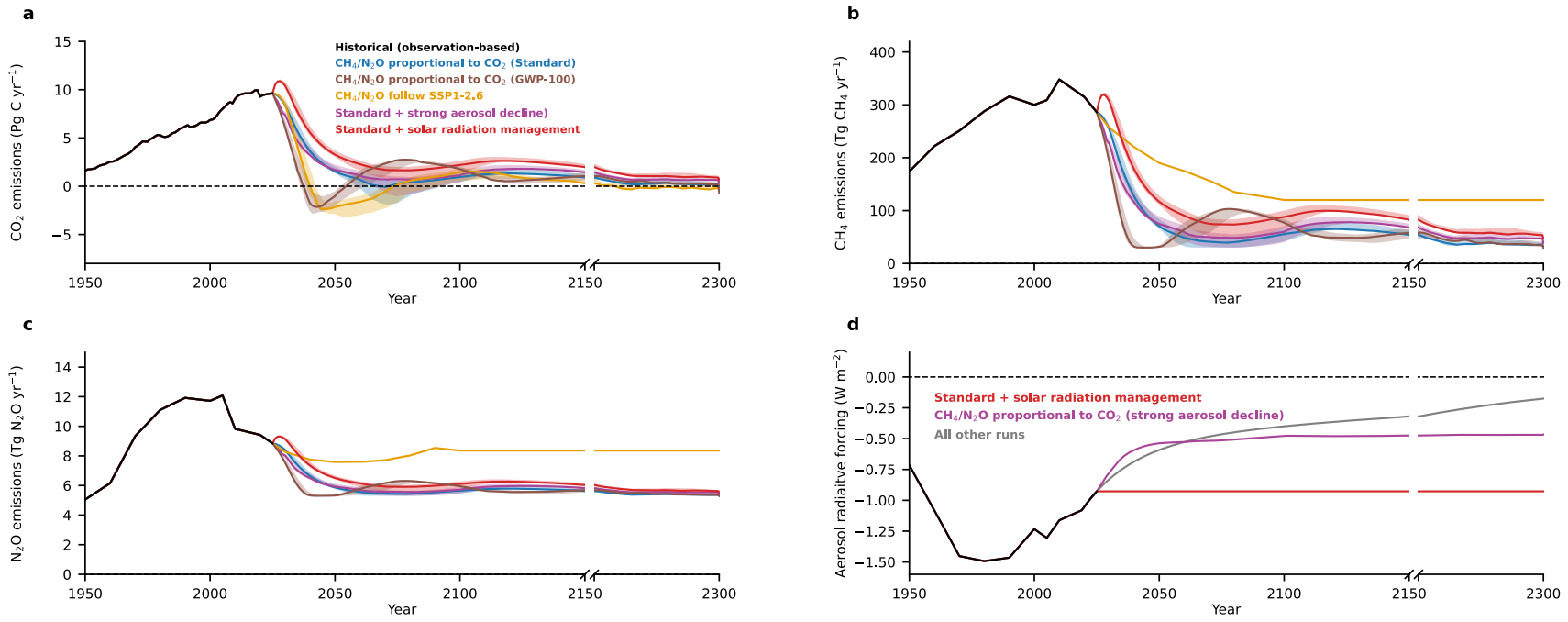

Fig. 3. Emissions of CO_2, CH_4, and N_2O, and aerosol radiative forcing following the adaptive emission reduction approach for the 1.5°C temperature target using different assumptions for non-CO_2 radiative forcing agents. (a) CO_2 emissions, **(b)** CH_4 emissions, **(c)** N_2O emissions, and **(d)** the total radiative forcing of anthropogenic aerosols (stratospheric and tropospheric) for five different idealized cases: aerosol radiative forcing decreases exponentially and CO_2, CH_4, and N_2O emissions evolve proportionally (blue), aerosol radiative forcing decreases exponentially and CO_2, CH_4, and N_2O emissions evolve proportionally but GWP-100 is used to split CO_2 equivalent emissions instead of the CO_2-fe approach (brown), aerosol radiative forcing decreases stronger due to strong CO_2 emissions cuts[71,72] and CO_2, CH_4, and N_2O emissions evolve proportionally (violet), aerosol radiative forcing decreases exponentially but CH_4, and N_2O emissions follow SSP1-2.6 after 2025 and only CO_2 evolves dynamically (ochre), and aerosol radiative forcing remains constant after 2025 and CO_2, CH_4, and N_2O emissions evolve proportionally (red, idealized solar radiation management). The thick solid lines show the average of the 8 simulations with varying magnitude and timing of

added inter-annual temperature variability of the Bern3D-LPX model configuration with an ECS of 3.2°C and the shaded area shows the range of all configurations that fall within the likely range of ECS as defined by Sherwood et al. (2020)[24]. The corresponding temperature curves, CO_2-fe emissions, and CO_2-e emissions for each simulated case are shown in Extended Data Figure 3.

The almost identical temperature curves and associated CO_2-fe emission curves across these four scenarios with varying CH_4, and N_2O emissions as well as varying radiative forcing from aerosols (Extended Data Figure 3) highlights the robustness of the CO_2-fe approach for transferring contributions from different radiative forcing agents to CO_2 equivalent emissions[7,15–17]. However, as the GWP-100 approach is widely used, e.g., in the Paris Agreement, we tested the AERA using GWP-100 by repeating the standard simulations but using the GWP-100 and not the CO_2-fe metric to transfer CH_4 and N_2O emissions to CO_2 equivalent emissions (brown curves in Figure 3). The AERA stabilizes the temperature at the given target when using GWP-100 (Extended Data Figure 5). However, the limitations[7,15,17–19] of the GWP-100 metric lead to an overcorrection at first of the CO_2, CH_4, and N_2O emissions reductions by the AERA by up to 78% for CO_2 (maximum relative difference in emissions reductions since 2025) and 46% for CH_4 and N_2O that is later corrected by positive CO_2-fe emissions (brown curves in Figure 3 and Extended Data Figure 5b-f). However, when the usage of GWP is envisioned, better results may be achieved by using temperature change potentials[70] or adjustments to the GWP over time[61].

The behavior of the AERA was further investigated assuming precautionary "over-compliance" (using a REB that is smaller than the central estimate, i.e., 67th and 83rd percentile instead of the 50th percentile) or "under-compliance" (using a REB that is higher than the central estimate, i.e., 17th and 33rd percentile). In the case of "under-compliance", the target temperature is still reached, but at the cost of a larger temperature overshoot (Extended Data Figures 6 and 7). In the case of "over-compliance", the temperature target is also reached, and the temperature overshoot can be avoided or reduced (for the highest ECS). Overall, the AERA thus provides a robust and working tool to estimate the necessary emission reductions to minimize the risk of temperature overshoot and the risk to surpass a given temperature limit, e.g., of 2^{o}C.

Applying the AERA in 2020

Having demonstrated the robustness and fidelity of the AERA in the model world, the question arises what rate of emission reductions the AERA would have estimated for the 1.5°C and 2.0°C temperature targets based on available observations and emissions statistics in 2020, when 186 parties had communicated their first NDCs to the United Nations Framework Convention on Climate Change (UNFCCC) Secretariat. Applied to observational data until 2020, step one of the AERA yields an anthropogenic warming of 1.23°C resulting in a remaining warming of 0.27°C for the 1.5°C target and 0.77°C for the 2.0°C target. In step 2, the ratio of the anthropogenic warming of 1.23°C and past cumulative CO_2-fe emissions of 749 Pg C results in an REB of 167 Pg C for 1.5°C and 472 Pg C for 2.0°C. These remaining CO_2-fe emissions are divided over the coming years in step 3 of the AERA assuming a cubic polynomial function with minimum changes of its slope. The so estimated reduction of annual CO_2-fe emissions from 2020 to 2025 is 3.7 Pg C for the 1.5°C temperature target (from 13.7 Pg C yr^{-1} in 2020 to 10.0 Pg C yr^{-1} in 2025) and 1.0 Pg C for the 2.0°C temperature target (from 13.7 Pg C yr^{-1} in 2020 to 12.6 Pg C yr^{-1} in 2025). Beyond 2025, CO_2-fe emissions would have to drop to 7.0 Pg C yr^{-1} in 2030 to reach the 1.5°C target, further decrease to 0.5 Pg C yr^{-1} in 2050 and become lightly negative after 2055 (up to -0.5 Pg C yr^{-1}) until reaching zero CO_2-fe emissions in 2085. For the 2.0°C target, CO_2-fe emissions would have to reach 11.3 Pg C yr^{-1} in 2030, 7.2 Pg C yr^{-1} in 2050 and zero CO_2-fe emissions by 2110. While the estimates of past warming, TCRE, REB, and necessary emission reductions have uncertainties, the AERA side-steps these uncertainties. The successive adaptation of the CO_2-fe emissions every five years allows to correct the emission pathway over time if the initial estimates were not exact. Estimates are based on the median (50^{th} percentile) value in these example calculations for year 2020. Other percentiles may be used, as in the "overcompliance case" described previously, for considering the precautionary principle of the UNFCCC.[71,72]

Discussion

The AERA allows estimating future CO_2-fe emission pathways to reach the desired temperature target within the uncertainty to which anthropogenic warming can be determined (±0.2°C)[26–29]. Climate projections by Earth System Models using the AERA could be incorporated into the periodical IPCC Assessment Reports and provide an alternative to the often-used approach of applying pre-defined emissions or concentration pathways (such as SSPs). Such pathways are generally designed a priori to be consistent with a given radiative forcing or warming level (e.g., SSP1-1.9 for 1.9 W m^{-2} and 1.5°C by 2100), not knowing the actual response of the Earth system to these emissions pathways[73]. AERA-based warming simulations from different models would be directly comparable in terms of impacts under equal warming. However, the sociotechnical feasibility of the pathways is not informed by the AERA but could be assessed by coupling these simulations to a cost-effectiveness integrative assessment model in a recursive dynamic setup. The approach may hence guide a valuable and highly policy-relevant complementary set of simulations for the next generation of CMIP models that result in a range of emission curves that all result in the same warming in the long term as opposed to current simulations with the same emission or concentration curves that can result in very different levels of warming.

In the Paris Agreement, the 2°C warming limit represents an upper threshold that should not be passed. The AERA applied with the median observation-based estimates allows to devise pathways that keep warming to within about 0.2°C of prescribed warming targets. For keeping warming below temperature limits that have been set as upper ceilings for global warming allowable to society, the AERA can be applied with a temperature target about 0.2°C lower than such limits or by using a lower than the median estimate for the REB as in the “overcompliance case”. In future efforts, the approach could be further

refined by applying the AERA within a fully observation-constrained probabilistic framework[12,13] to estimate the necessary emission reductions with associated likelihoods.

The AERA presents policy makers transparent science- and observation-based emission reductions that would be necessary to limit global warming to any chosen temperature level without the need to make climate projections with Earth System Models. With many simulations, substituting for future real-world outcomes, we have shown that this approach is robust across a vast number of possible developments. Policy makers may wish to use the information from the AERA to regularly update near- and long-term emission reduction goals, including additional socio-economic considerations such as equity, mitigation versus adaptation costs, and risks of not meeting a target. The AERA can thereby help to successfully "keep global warming well below 2°C and to pursue efforts to limit it to 1.5°C"[6].

Data availability

The Bern3D-LPX model output is available publicly available via SEANOE (https://doi.org/10.17882/90901)[74]. All other data are available in the main text or the supplementary materials.

Code availability

The AERA code is publicly available via https://github.com/Jete90/AERA[75].

Acknowledgements

We thank Piers Forster, Joeri Rogelj, and an unknown reviewer for their valuable comments. This work was funded by the European Union's Horizon 2020 research and innovation programme under grant agreement No 821003 (project 4C, Climate-Carbon Interactions in the Current Century) (JT, TLF, FJ, PF), and grant agreement No 101003687 (project PROVIDE, Paris Agreement Overshooting) (TLF), and by the Swiss National Science Foundation under grant PP00P2_198897 (TLF) and grant #200020_200511 (FJ). The work reflects only the authors' view; the European Commission and their executive agency are not responsible for any use that may be made of the information the work contains. We thank Damien Guignet for initial analysis, Sebastian Lienert and Aurich Jeltsch-Thömmes for help with Bern3D-LPX, and the 4C partners for helpful discussions.

Author Contributions

Conceptualization: JT, TLF, FJ, PF

Methodology: JT, MA, TLF, FJ

Software: JT, MA

Investigation: JT

Visualization: JT, TLF, FJ

Funding acquisition: TLF, FJ, PF

Project administration: TLF, FJ

Writing – original draft: JT

Writing – review & editing: JT, MA, TLF, FJ, PF

Author information/Competing Interests

Authors declare that they have no competing interests.

References

1. World Meteorological Organization. *State of the Global Climate 2020*. https://library.wmo.int/doc_num.php?explnum_id=10618 (2021).
2. Allen, M. R. *et al.* Framing and Context. in *Global warming of 1.5°C* (eds. Masson-Delmotte, V. et al.) (2018).
3. IPCC. *Special Report on the Ocean and Cryosphere in a Changing Climate*. (2019).
4. Hoegh-Guldberg, O. *et al.* The human imperative of stabilizing global climate change at 1.5°C. *Science (1979)* **365**, eaaw6974 (2019).
5. Hoegh-Guldberg, O. *et al.* Impacts of 1.5°C of Global Warming on Natural and Human Systems. in *Global warming of 1.5°C* (eds. Masson-Delmotte, V. et al.) (2018).
6. UNFCCC. *Paris agreement. Report of the Conference of the Parties to the United Nations Framework Convention on Climate Change*. (2015).
7. Jenkins, S., Millar, R. J., Leach, N. & Allen, M. R. Framing Climate Goals in Terms of Cumulative CO2-Forcing-Equivalent Emissions. *Geophys Res Lett* **45**, 2795–2804 (2018).
8. Rogelj, J., Forster, P. M., Kriegler, E., Smith, C. J. & Séférian, R. Estimating and tracking the remaining carbon budget for stringent climate targets. *Nature* **571**, 335–342 (2019).
9. Matthews, H. D. *et al.* Opportunities and challenges in using remaining carbon budgets to guide climate policy. *Nat Geosci* **13**, 769–779 (2020).
10. Tokarska, K. B. & Gillett, N. P. Cumulative carbon emissions budgets consistent with 1.5 °C global warming. *Nat Clim Chang* **8**, 296–299 (2018).
11. Peters, G. P. Beyond carbon budgets. *Nat Geosci* **11**, 378–380 (2018).
12. Damon Matthews, H. *et al.* An integrated approach to quantifying uncertainties in the remaining carbon budget. *Commun Earth Environ* **2**, 7 (2021).
13. Steinacher, M., Joos, F. & Stocker, T. F. Allowable carbon emissions lowered by multiple climate targets. *Nature* **499**, 197–201 (2013).
14. IPCC. Summary for Policymakers. in *Climate Change 2013: The Physical Science Basis.Contribution of Working Group I to the Fifth Assessment Report of the Intergovernmental Panel on Climate Change* (eds. Stocker, T. F. et al.) (Cambridge University Press, 2013).
15. Allen, M. R. *et al.* A solution to the misrepresentations of CO2-equivalent emissions of short-lived climate pollutants under ambitious mitigation. *NPJ Clim Atmos Sci* **1**, 16 (2018).

16. Wigley, T. M. L. The Kyoto Protocol: CO2 CH4 and climate implications. *Geophys Res Lett* **25**, 2285–2288 (1998).
17. Smith, M. A., Cain, M. & Allen, M. R. Further improvement of warming-equivalent emissions calculation. *NPJ Clim Atmos Sci* **4**, 19 (2021).
18. Tanaka, K. & O'Neill, B. C. The Paris Agreement zero-emissions goal is not always consistent with the 1.5 °C and 2 °C temperature targets. *Nat Clim Chang* **8**, 319–324 (2018).
19. Allen, M. *et al.* Ensuring that offsets and other internationally transferred mitigation outcomes contribute effectively to limiting global warming. *Environmental Research Letters* **16**, 74009 (2021).
20. *Paragraphs 37 of the Addendum to UNFCCC Decision 18/CMA.1, agreed at the COP24 in December 2018*.
21. Arias, P. A. *et al.* Technical Summary. in *Climate Change 2021: The Physical Science Basis. Contribution of Working Group I to the Sixth Assessment Report of the Intergovernmental Panel on Climate Change* (eds. Masson-Delmotte, V. et al.) (Cambridge University Press, 2021).
22. A, M. G. *et al.* Context for interpreting equilibrium climate sensitivity and transient climate response from the CMIP6 Earth system models. *Sci Adv* **6**, eaba1981 (2022).
23. Nijsse, F. J. M. M., Cox, P. M. & Williamson, M. S. Emergent constraints on transient climate response (TCR) and equilibrium climate sensitivity (ECS) from historical warming in CMIP5 and CMIP6 models. *Earth System Dynamics* **11**, 737–750 (2020).
24. Sherwood, S. C. *et al.* An Assessment of Earth's Climate Sensitivity Using Multiple Lines of Evidence. *Reviews of Geophysics* **58**, e2019RG000678 (2020).
25. Tokarska Katarzyna, B. *et al.* Past warming trend constrains future warming in CMIP6 models. *Sci Adv* **6**, eaaz9549 (2021).
26. Haustein, K. *et al.* A real-time Global Warming Index. *Sci Rep* **7**, 15417 (2017).
27. Ribes, A., Qasmi, S. & Gillett, N. P. Making climate projections conditional on historical observations. *Sci Adv* **7**, eabc0671 (2022).
28. Gillett, N. P. *et al.* Constraining human contributions to observed warming since the pre-industrial period. *Nat Clim Chang* **11**, 207–212 (2021).
29. IPCC. Summary for Policymakers. in *Climate Change 2021: The Physical Science Basis. Contribution of Working Group I to the Sixth Assessment Report of the Intergovernmental*

Panel on Climate Change (eds. Masson-Delmotte, V. et al.) (Cambridge University Press, 2021).

30. MacDougall, A. H. *et al.* Is there warming in the pipeline? A multi-model analysis of the Zero Emissions Commitment from CO_2. *Biogeosciences* **17**, 2987–3016 (2020).
31. Saunois, M. *et al.* The Global Methane Budget 2000–2017. *Earth Syst Sci Data* **12**, 1561–1623 (2020).
32. Heinze, C. *et al.* ESD Reviews: Climate feedbacks in the Earth system and prospects for their evaluation. *Earth System Dynamics* **10**, 379–452 (2019).
33. Friedlingstein, P. *et al.* Global Carbon Budget 2020. *Earth Syst Sci Data* **12**, 3269–3340 (2020).
34. Arora, V. K. *et al.* Carbon–concentration and carbon–climate feedbacks in CMIP6 models and their comparison to CMIP5 models. *Biogeosciences* **17**, 4173–4222 (2020).
35. Jones, C. D. & Friedlingstein, P. Quantifying process-level uncertainty contributions to TCRE and carbon budgets for meeting Paris Agreement climate targets. *Environmental Research Letters* **15**, 074019 (2020).
36. Tian, H. *et al.* A comprehensive quantification of global nitrous oxide sources and sinks. *Nature* **586**, 248–256 (2020).
37. Thompson, D. W. J., Wallace, J. M., Jones, P. D. & Kennedy, J. J. Identifying Signatures of Natural Climate Variability in Time Series of Global-Mean Surface Temperature: Methodology and Insights. *J Clim* **22**, 6120–6141 (2009).
38. Medhaug, I., Stolpe, M. B., Fischer, E. M. & Knutti, R. Reconciling controversies about the 'global warming hiatus'. *Nature* **545**, 41–47 (2017).
39. Turner, J. *et al.* Absence of 21st century warming on Antarctic Peninsula consistent with natural variability. *Nature* **535**, 411–415 (2016).
40. Watanabe, M. *et al.* Strengthening of ocean heat uptake efficiency associated with the recent climate hiatus. *Geophys Res Lett* **40**, 3175–3179 (2013).
41. Peters, G. P. *et al.* Towards real-time verification of CO2 emissions. *Nat Clim Chang* **7**, 848–850 (2017).
42. Spring, A., Ilyina, T. & Marotzke, J. Inherent uncertainty disguises attribution of reduced atmospheric CO2 growth to CO2 emission reductions for up to a decade. *Environmental Research Letters* **15**, 114058 (2020).

43. Steffen, W. *et al.* Trajectories of the Earth System in the Anthropocene. *Proceedings of the National Academy of Sciences* **115**, 8252 (2018).
44. Oppenheimer, M., O'Neill, B. C. & Webster, M. Negative learning. *Clim Change* **89**, 155–172 (2008).
45. Webster, M., Jakobovits, L. & Norton, J. Learning about climate change and implications for near-term policy. *Clim Change* **89**, 67–85 (2008).
46. Otto, F. E. L., Frame, D. J., Otto, A. & Allen, M. R. Embracing uncertainty in climate change policy. *Nat Clim Chang* **5**, 917–920 (2015).
47. Held, I. M. *et al.* Probing the Fast and Slow Components of Global Warming by Returning Abruptly to Preindustrial Forcing. *J Clim* **23**, 2418–2427 (2010).
48. Joos, F. *et al.* Carbon dioxide and climate impulse response functions for the computation of greenhouse gas metrics: a multi-model analysis. *Atmos Chem Phys* **13**, 2793–2825 (2013).
49. Enting, I. G. On the use of smoothing splines to filter CO2 data. *Journal of Geophysical Research: Atmospheres* **92**, 10977–10984 (1987).
50. Luo, J., Ying, K. & Bai, J. Savitzky–Golay smoothing and differentiation filter for even number data. *Signal Processing* **85**, 1429–1434 (2005).
51. Allen, M. R. *et al.* Warming caused by cumulative carbon emissions towards the trillionth tonne. *Nature* **458**, 1163–1166 (2009).
52. Matthews, H. D., Gillett, N. P., Stott, P. A. & Zickfeld, K. The proportionality of global warming to cumulative carbon emissions. *Nature* **459**, 829–832 (2009).
53. IPCC. Summary for Policymakers. in *Climate Change 2014: Synthesis Report. Contribution of Working Groups I, II and III to the Fifth Assessment Report of the Intergovernmental Panel on Climate Change* (eds. Pachauri, R. K. & Meyer, L. A.) (IPCC, 2014).
54. Edwards, M. R., McNerney, J. & Trancik, J. E. Testing emissions equivalency metrics against climate policy goals. *Environ Sci Policy* **66**, 191–198 (2016).
55. Ricke, K. L., Millar, R. J. & MacMartin, D. G. Constraints on global temperature target overshoot. *Sci Rep* **7**, 14743 (2017).
56. Parry, M., Lowe, J. & Hanson, C. Overshoot, adapt and recover. *Nature* **458**, 1102–1103 (2009).
57. Anderson, C. M. *et al.* Planning for Change: Conservation-Related Impacts of Climate Overshoot. *Bioscience* **70**, 115–118 (2020).

58. de Vrese, P. & Brovkin, V. Timescales of the permafrost carbon cycle and legacy effects of temperature overshoot scenarios. *Nat Commun* **12**, 2688 (2021).
59. Myhre, G. *et al.* Anthropogenic and Natural Radiative Forcing. in *Climate Change 2013: The Physical Science Basis. Contribution of Working Group I to the Fifth Assessment Report of the Intergovernmental Panel on Climate Change* (eds. Stocker, T. F. et al.) (Cambridge University Press, 2013).
60. Harmsen, M. J. H. M. *et al.* How climate metrics affect global mitigation strategies and costs: a multi-model study. *Clim Change* **136**, 203–216 (2016).
61. Tanaka, K., Boucher, O., Ciais, P., Johansson, D. J. A. & Morfeldt, J. Cost-effective implementation of the Paris Agreement using flexible greenhouse gas metrics. *Sci Adv* **7**, eabf9020 (2022).
62. Roth, R., Ritz, S. P. & Joos, F. Burial-nutrient feedbacks amplify the sensitivity of atmospheric carbon dioxide to changes in organic matter remineralisation. *Earth System Dynamics* **5**, 321–343 (2014).
63. Lienert, S. & Joos, F. A Bayesian ensemble data assimilation to constrain model parameters and land-use carbon emissions. *Biogeosciences* **15**, 2909–2930 (2018).
64. Joos, F. *et al.* Global warming feedbacks on terrestrial carbon uptake under the Intergovernmental Panel on Climate Change (IPCC) Emission Scenarios. *Global Biogeochem Cycles* **15**, 891–907 (2001).
65. Climate Action Tracker . https://climateactiontracker.org/documents/853/CAT_2021-05-04_Briefing_Global-Update_Climate-Summit-Momentum.pdf.
66. Meinshausen, M. *et al.* Realization of Paris Agreement pledges may limit warming just below 2 °C. *Nature* **604**, 304–309 (2022).
67. Wigley, T. M. L. The relationship between net GHG emissions and radiative forcing with an application to Article 4.1 of the Paris Agreement. *Clim Change* **169**, 13 (2021).
68. Wigley, T. M. L. A Combined Mitigation/Geoengineering Approach to Climate Stabilization. *Science (1979)* **314**, 452–454 (2006).
69. Robock, A., Oman, L. & Stenchikov, G. L. Regional climate responses to geoengineering with tropical and Arctic SO2 injections. *Journal of Geophysical Research: Atmospheres* **113**, (2008).
70. Shine, K. P., Berntsen, T. K., Fuglestvedt, J. S., Skeie, R. B. & Stuber, N. Comparing the climate effect of emissions of short- and long-lived climate agents. *Philosophical*

Transactions of the Royal Society A: Mathematical, Physical and Engineering Sciences **365**, 1903–1914 (2007).

71. Rogelj, J. *et al.* Air-pollution emission ranges consistent with the representative concentration pathways. *Nat Clim Chang* **4**, 446–450 (2014).

72. Lamboll, R. D., Nicholls, Z. R. J., Kikstra, J. S., Meinshausen, M. & Rogelj, J. Silicone v1.0.0: an open-source Python package for inferring missing emissions data for climate change research. *Geosci Model Dev* **13**, 5259–5275 (2020).

73. O'Neill, B. C. *et al.* The Scenario Model Intercomparison Project (ScenarioMIP) for CMIP6. *Geosci Model Dev* **9**, 3461–3482 (2016).

74. Terhaar, J., Frölicher, T. L., Aschwanden, M. & Joos, F. Bern3D-LPX simulations with the the adaptive emission reduction approach (AERA). SEANOE. https://doi.org/10.17882/90901

75. Terhaar, J., Frölicher, T. L., Aschwanden, M. & Joos, F. Adaptive emission reduction approach (AERA). Preprint at https://doi.org/10.5281/zenodo.7186275 (2022).

Methods

Adaptive Emission Reduction Approach

The Adaptive Emission Reduction Approach (AERA)[75] is designed to estimate a future trajectory of CO_2 forcing equivalent (CO_2-fe) emissions to reach a temperature target. The AERA is formulated as part of a control system with a feedback loop. In a control system, the output of a system is controlled by regularly adjusting the input to the system based on the deviation between the actual and target value of a process variable. An example is a regulation of room temperature with a heating-cooling unit. The room temperature is measured to estimate the deviation between the actual and target temperature. The flow of heat between the unit and the room is then adjusted by the "controller" based on the deviation and the median available estimate of the response in room temperature to heat flow. This procedure is repeated, e.g., every minute, to adjust the room temperature towards and to track the target temperature. Similarly, the AERA, when implemented with real-world emissions, will control the evolution of anthropogenic warming by adjusting CO_2-fe emissions. Here, emissions are foreseen to be adjusted every five years, based on the median observational estimate of the deviation between actual and target anthropogenic warming and the median observation-based estimate of the Earth system's response to emissions. Implementing the regularly updated emissions reductions following the AERA will allow the temperature to converge towards the target temperature, despite uncertainties in our understanding of the Earth System.

As input, the AERA requires past global time-series of three variables: (i) global mean surface temperature (GMST), (ii) total anthropogenic radiative forcing (RF), and (iii) total CO_2-fe emissions from CO_2, non-CO_2 GHGs, precursors, aerosols, and land-use change combined (see CO_2-fe emissions calculation below). The

AERA contains three steps. First, internal variability from the GMST record is removed by calculating anthropogenic warming from the GMST timeseries[46]. Second, the Remaining CO_2-fe Emission Budget (REB)[2,7–9] is estimated based on the near-linear relationship between past CO_2-fe emissions and warming (i.e., the transient climate response to cumulative carbon emission)[51,52], and the remaining temperature gap before the target temperature will be reached. Third, this REB is distributed over the future years using a cubic polynomial function. The three steps are to be repeated every five years. Therefore, the future CO_2-fe emission curve may be adjusted every five years based on the most up-to-date observations of GMST, RF, and CO_2-fe emissions.

In the first step, the natural internal and external (i.e., volcanoes, solar activity) variability is removed from the observed, historical GMST resulting in a temperature curve (T_{ant}) that only changes due to anthropogenic forcing. T_{ant} is determined following Otto et al.[46] by fitting an Impulse-Response Function (IRF)[47,48] to the observed GMST(t). The IRF features three characteristic timescales, τ_i, and coefficients, a_i:

$$T_{ant}(t) = T_{ant}(1850) + c \int_{1850}^{t} I_{RF}(t') \left(a_1 \left(1 - e^{\frac{-(t-t')}{\tau_1}}\right) + a_2 \left(1 - e^{\frac{-(t-t')}{\tau_2}}\right) + a_3 \left(1 - e^{\frac{-(t-t')}{\tau_3}}\right) \right) dt' \quad (1)$$

Eq. 1 relates the sum of step-like changes in RF (impulses $I_{RF}(t')$, defined as the change in RF in year t') over the past observed period to $T_{ant}(t)$. The constant c is a scaling and unit conversion factor, and the integral is approximated by the sum of annual values. The seven free parameters of Eq. 1 *(timescales* τ_1, τ_2, and τ_3*; coefficients* a_1, a_2*; c;* T_{ant} *(1850)* are determined to best fit the observation-based GMST by minimizing the root-mean-square-deviations between $T_{ant}(t)$ and *GMST(t).* The parameters are determined at each stocktake to account for possible feedbacks from the warming of the climate and cumulative CO_2 uptake that may change the shape of the IRF[76]. The free parameters were constrained a priori to ease the fitting.

The timescales are limited to 1.5-2.0 years (for τ_1), 15-30 years (τ_2), and 100-600 years (τ_3) and the coefficients are limited to 0.2-0.4 (a_1), 0.3-0.5 (a_2). a_3 is calculated by $a_3 = 1 - a_1 - a_2$. Implicitly, a_3 is thus limited to 0.1-0.5. These broad constraints are enforced to ensure physically meaningful parameters. From the anthropogenic temperature time-series $T_{ant}(t)$, the anthropogenic temperature anomaly (ΔT_{ant}) is calculated by subtracting the mean *GMST(t)* over the reference period 1850-1900 from T_{ant}:

$$\Delta T_{ant}(t) = T_{ant}(t) - \overline{GMST(1850-1900)} \quad (2)$$

The Remaining Emission Budget (REB) of CO_2-fe emissions is estimated at the time of the stocktake, t_{st} (years 2025, 2030, …) exploiting the near-linearity between warming and cumulative CO_2 emissions discussed by the Intergovernmental Panel on Climate Change[14,53]. The REB (t_{st}) is determined by multiplying the remaining anthropogenic temperature anomaly until the target temperature is reached with the ratio of cumulative CO_2-fe emissions since 1850 ($\int_{1850}^{t_{st}} E_{fe}^{CO_2}(t')dt'$) and the realized anthropogenic warming anomaly $\Delta T_{ant}(t_{st})$[51,52]:

$$REB(t_{st}) = \left(\Delta T_{ant}^{target} - \Delta T_{ant}(t_{st})\right) \frac{\int_{1850}^{t_{st}} E_{fe}^{CO_2}(t')dt'}{\Delta T_{ant}(t_{st})}, \quad (3)$$

with ΔT_{ant}^{target} being the temperature target, e.g., 1.5°C or 2°C.

The emission pathway for the five years following the stocktake is determined by distributing the remaining CO_2-fe emission budget over the future years using a cubic polynomial function:

$$E_{fe}^{CO_2}(t) = at^3 + bt^2 + ct + d \qquad \text{for } t_{target} \geq t \geq t_{st}\ , \quad (4)$$

with t referring to the time after the year of the stocktake (t_{st}) and t_{target} being the year when the temperature target should be reached. The t_{target} is not an a priori fixed year[61,70] but continuous to evolve over time and will be adapted here to ensure that the change of the slope of CO_2-fe emissions remains as small as possible (see paragraph below). The parameters *a*, *b*, *c*, and *d* are chosen to determine an emission curve with a small curvature using the following boundary conditions:

1) $E_{fe}^{CO_2}(t_{st})$ equals the CO_2-fe emissions at the year of the stocktake.

2) Changes in $E_{fe}^{CO_2}$ in the year before the stocktake are as close as possible to changes in $E_{fe}^{CO_2}$ at the year of the stocktake:

$$\frac{\partial E_{fe}^{CO_2}}{\partial t}(t_{st}) = \frac{\partial E_{fe}^{CO_2}}{\partial t}(t_{st} - 1) + \eta, \quad (5)$$

with η being a change in the slope.

3) $E_{fe}^{CO_2}(t_{target})$ equals zero.

4) $E_{fe}^{CO_2}$ remains constant after the target year is reached ($\frac{\partial E_{fe}^{CO_2}}{\partial t}(t_{target}) = 0$)

Condition 1) enforces the polynomial function to match emissions at the time of the stocktake. Condition 2) minimizes the changes in the emissions trend around the stocktake, thereby implicitly accounting for inertia in the socio-economic system that makes it difficult to 'abruptly' change trends. Conditions 3) and 4) imply that CO_2-fe emissions are zero when the target is reached and stay zero afterward in the absence of any trend change in emissions. These boundary conditions leave two free parameters t_{target} and η. For each combination of these two parameters one emission curve exists. The maximum length of the time

series (t_{max}) varies dynamically depending on the REB and the CO_2-fe emissions in the year of the stocktake:

$$t_{max} = 30yr + 90yr \times e^{\left(-\frac{|max(REB-30\ Pg\ C,\ \ 0\ Pg\ C)|}{50\ Pg\ C}\right)} + min\left(\left|E^{*CO_2}_{fe}\ (t_{st})\right|,\ 10\ \frac{Pg\ C}{yr}\right)^2 \times \frac{yr^3}{(Pg\ C)^2}. \quad (6)$$

Each term in equation (6) is rounded to its nearest integer. This dynamic definition keeps the time until which the temperature target should be reached (t_{max}) relatively short (close to 30 years, first term in equation (6)) so that the temperature does not remain off target for too long. However, in two cases, it is preferable that the REB is distributed over a longer time. The first case occurs when the anthropogenic warming is close to the temperature target. In that case, a short t_{max} leads to abrupt short-term changes in CO_2-fe emissions because a small REB (< ~100 Pg C) is forced into a small number of years (Supplementary Figure 1). To avoid such an oscillation, t_{max} increases by up to additional 90 years when the REB becomes small (term 2 in equation (6)). The second case occurs when the REB is large, but annual emissions are still high (> ~5 Pg C yr^{-1}). These high emissions will already be correcting the temperatures over time. A reduced t_{max} would force the large REB into a small number of years, and cause even higher emissions in the first years, which need to be reduced shortly afterwards (Supplementary Figure 1). The third term in equation (6), with $E^{*CO_2}_{fe}\ (t_{st})$ being equal to $E^{CO_2}_{fe}\ (t_{st})$ if the REB and $E^{CO_2}_{fe}\ (t_{st})$ have the same sign and being zero otherwise, increases t_{max} by up to 100 years. Overall, the choice of the different timescales does not rely on theoretical assumptions, but it is a result of tests across a wide range of timescales.

For determining the free parameters t_{target} and η, we systematically varied them in steps of 1 year and 0.1 Pg C yr^{-2} within the following limits: 5 years < (t_{target}-t_{st}) < t_{max} ; -2.5 Pg C yr^{-2} < η < 2.5 Pg C yr^{-2}. The 'best' choice out of these emission curves is chosen in three steps:

First, all curves are excluded whose integrated emissions from t_{st} to t_{target} do not agree with the REB within ± 5 Pg C ($|\xi| < 5$ Pg C):

$$\xi = \int_{t_{st}}^{t_{target}} E_{fe}^{CO_2}(t')dt' - REB, \quad (7)$$

with ξ being the difference between the REB and the integral of the CO_2-fe emission curve. In our tests, at every stocktake at least one CO_2-fe emissions curve with a REB that lies within ±5 Pg C of the REB determined by the AERA is found. In the potential cases where a curve within the REB limit cannot be found, the curve with the smallest $|\xi|$ would be chosen.

Second, among the remaining curves, all curves are excluded with exceedance emissions (ε) being larger than 10 Pg C. Exceedance emissions are defined as follows:

$$\int_{t_{st}}^{t_{target}} \left|E_{fe}^{CO_2}(t')\right| dt' - \int_{t_{st}}^{t_{target}} E_{fe}^{CO_2}(t')dt' < 2\varepsilon \quad (8)$$

The left side of equation (8) describes the difference between the integral of the absolute emissions over time and the emissions integral. Although this difference is ideally zero, it can diverge if $E_{fe}^{CO_2}(t')$ changes its sign between t_{st} and t_{target}. This can for example be the case if $E_{fe}^{CO_2}(t_{st})$ is still positive and $T_{ant}(t_{st})$ is already larger than the temperature target. Thus, the still emitted positive emissions before emissions become negative increase the exceedance of T_{ant} further and are therefore called 'exceedance emissions'. They are later compensated by the roughly similar amount of negative emissions, hence the factor 2 on the right side of equation (8). Several studies[77–80] have shown that the global warming response to positive and negative CO_2 emissions is indeed approximately symmetrical for moderate amounts of negative emissions and under ambitious climate targets.

In 99.95% of the cases a CO_2-fe emissions curve with exceedance emissions smaller than 10 Pg C is found. In the remaining 0.05% cases, the curve with the smallest exceedance emissions is chosen. In the 99.95% of the cases where the limits for $|\xi|$ and exceedance emissions are met, the curve is retained with the combination of t_{target} and η that results in the smallest curvature (sum of absolute changes in emissions change). The smallest curvature is calculated by minimizing the sum of each curve's (absolute) second derivates from year t_{st}*-1* to year t_{target}.

CO_2-fe emissions from non-CO_2 agents

The historical CO_2-fe emissions from non-CO_2 agents are estimated based on the radiative forcing time-series of non-CO_2 agents. This annual time series is translated into CO_2-fe emissions[17]:

$$\alpha E_{CO_2-fe}(t) = \frac{dF_{non-CO_2}(t)}{dt} + \rho F_{non-CO_2}(t)\,, \quad (9)$$

with F_{non-CO_2} (t) being the radiative forcing of non-CO_2 agents, $E_{CO_2-fe}(t)$ being CO_2-fe emissions from non-CO_2 agents, with ρ being the rate of decline of radiative forcing over these timescales under zero emissions (0.33%), and α being a constant representing the forcing impact of ongoing CO_2 emissions (1.08 W m^{-2} per 1,000 $GtCO_2$).

Applying the AERA to observations until 2020

The necessary emission reductions in 2020 are quantified using the AERA. As input, we used the historical GMST data from HadCRUT5 (https://crudata.uea.ac.uk/cru/data/temperature/), historical CO_2 concentrations from Meinshausen et al. (2017)[81] until 2014 and from NOAA GML from 2015 to 2020 (https://gml.noaa.gov/webdata/ccgg/trends/co2/co2_annmean_gl.txt), historical radiative forcing from

726 non-CO_2 radiative agents from the RCP database, assuming RCP2.6 from 2005 to 2020
727 (https://tntcat.iiasa.ac.at/RcpDb/dsd?Action=htmlpage&page=welcome)[82–90], historical CO_2 fossil fuel
728 and land-use change emissions from the Global Carbon Project[33], and historical CO_2-fe emissions from
729 non-CO_2 forcing agents derived from the non-CO_2 radiative forcing from the RCP database.
730
731 The estimated warming in 2020, past cumulative CO_2-fe emissions, and the remaining CO_2-fe emissions
732 budgets to limit global warming to 1.5°C and 2°C and the estimated time when zero CO_2-fe emissions need
733 to be reached based on this data lie within previous estimates. Previous estimates of the anthropogenic
734 warming are 1.0 ± 0.2°C in 2017[2], 1.07 (0.8-1.3)°C for the period from 2010-2019[29], and 1.20°C in 2020[26].
735 In comparison, the AERA-derived temperature is 1.15°C in 2017, 1.08°C from 2010 to 2019, and 1.23 in
736 2020, in agreement with the three previous estimates. The resulting remaining CO_2-fe budget, when
737 scaled to the remaining warming in 2020 (0.27°C), was estimated to be 117–270 Pg C[7,21]. This estimation
738 encompasses the here presented REB estimate of 168 Pg C.
739
740 Supplementary Methods
741
742 Additional information about the methods that are used throughout this study is made available as
743 Supplementary Information. The Supplementary Information includes a detailed description of the AERA
744 testing wit Bern3D-LPX, the reduced form atmospheric chemistry model, and the AERA robustness tests.
745
746

References – Methods

76. Millar, R. J., Nicholls, Z. R., Friedlingstein, P. & Allen, M. R. A modified impulse-response representation of the global near-surface air temperature and atmospheric concentration response to carbon dioxide emissions. *Atmos Chem Phys* **17**, 7213–7228 (2017).

77. Palter, J. B., Frölicher, T. L., Paynter, D. & John, J. G. Climate, ocean circulation, and sea level changes under stabilization and overshoot pathways to 1.5K warming. *Earth System Dynamics* **9**, 817–828 (2018).

78. Koven, C. *et al.* 23rd Century surprises: Long-term dynamics of the climate and carbon cycle under both high and net negative emissions scenarios. *Earth System Dynamics Discussions* **2021**, 1–32 (2021).

79. Zickfeld, K., MacDougall, A. H. & Matthews, H. D. On the proportionality between global temperature change and cumulative CO 2 emissions during periods of net negative CO 2 emissions. *Environmental Research Letters* **11**, 055006 (2016).

80. Tokarska, K. B., Zickfeld, K. & Rogelj, J. Path Independence of Carbon Budgets When Meeting a Stringent Global Mean Temperature Target After an Overshoot. *Earths Future* **7**, 1283–1295 (2019).

81. Meinshausen, M. *et al.* Historical greenhouse gas concentrations for climate modelling (CMIP6). *Geosci Model Dev* **10**, 2057–2116 (2017).

82. van Vuuren, D. P. *et al.* Stabilizing greenhouse gas concentrations at low levels: an assessment of reduction strategies and costs. *Clim Change* **81**, 119–159 (2007).

83. Schultz, M. G. *et al.* Global wildland fire emissions from 1960 to 2000. *Global Biogeochem Cycles* **22**, (2008).

84. Mieville, A. *et al.* Emissions of gases and particles from biomass burning during the 20th century using satellite data and an historical reconstruction. *Atmos Environ* **44**, 1469–1477 (2010).

85. Eyring, V. *et al.* Transport impacts on atmosphere and climate: Shipping. *Atmos Environ* **44**, 4735–4771 (2010).

86. Lee, D. S. *et al.* Aviation and global climate change in the 21st century. *Atmos Environ* **43**, 3520–3537 (2009).

87. Lamarque, J.-F. *et al.* Historical (1850–2000) gridded anthropogenic and biomass burning emissions of reactive gases and aerosols: methodology and application. *Atmos Chem Phys* **10**, 7017–7039 (2010).
88. Hurtt, G. C. *et al.* Harmonization of land-use scenarios for the period 1500–2100: 600 years of global gridded annual land-use transitions, wood harvest, and resulting secondary lands. *Clim Change* **109**, 117 (2011).
89. Smith, S. J., Pitcher, H. & Wigley, T. M. L. Global and regional anthropogenic sulfur dioxide emissions. *Glob Planet Change* **29**, 99–119 (2001).
90. Bond, T. C. *et al.* Historical emissions of black and organic carbon aerosol from energy-related combustion, 1850–2000. *Global Biogeochem Cycles* **21**, (2007).

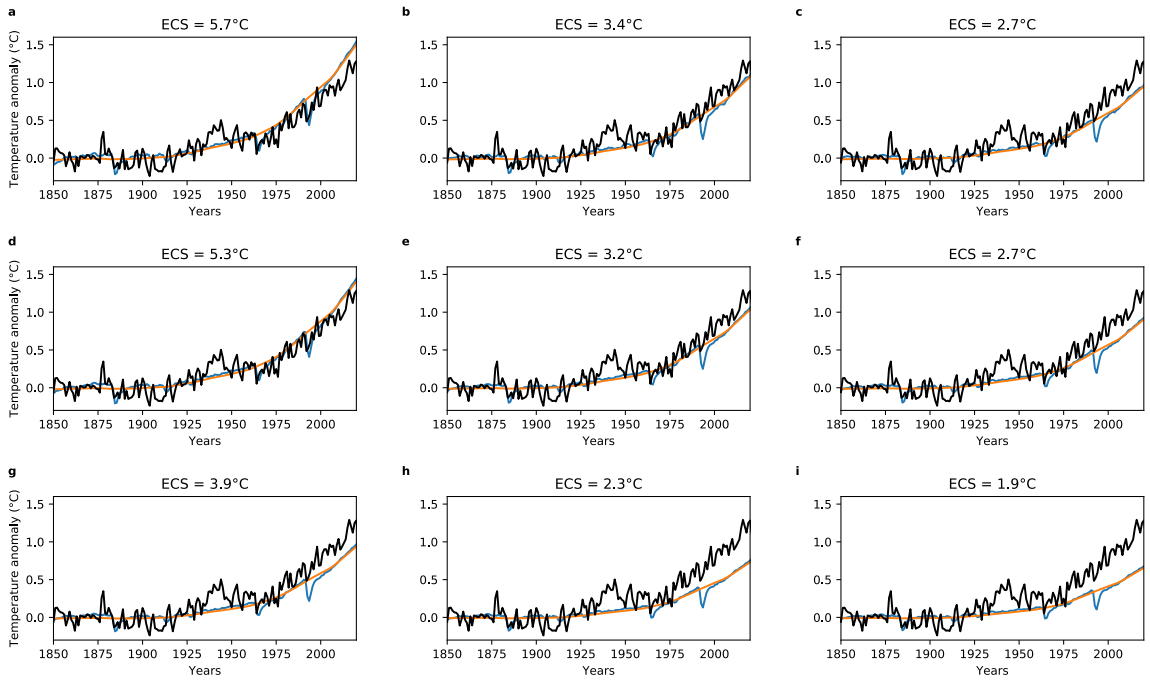

789

790 **Extended Data Figure 1. Historical and simulated globally averaged surface atmospheric**
791 **temperature anomaly with respect to 1850-1900 for different model configurations. (a-i)** Global
792 mean surface temperature (GMST) from 1850 to 2020 for 9 model configurations with varying ECS
793 without the superimposed inter-annual variability. The blue lines show the simulated GMST, and the
794 orange lines show the determined anthropogenic warming. The diapycnal diffusivity coefficients are
795 $1x10^{-5}$, $2x10^{-5}$ and $1x10^{-4}$ m^2 s^{-1} (from top to bottom) and the different numbers for the internal Bern3D
796 model parameter that accounts for climate feedbacks, which are not explicitly represented in the
797 model, are 0.1, -0.5, and -0.8 W m^{-2} K^{-1} (from left to right). The HadCRUT5 observation-based GMST
798 time-series is shown in black in all panels.

799

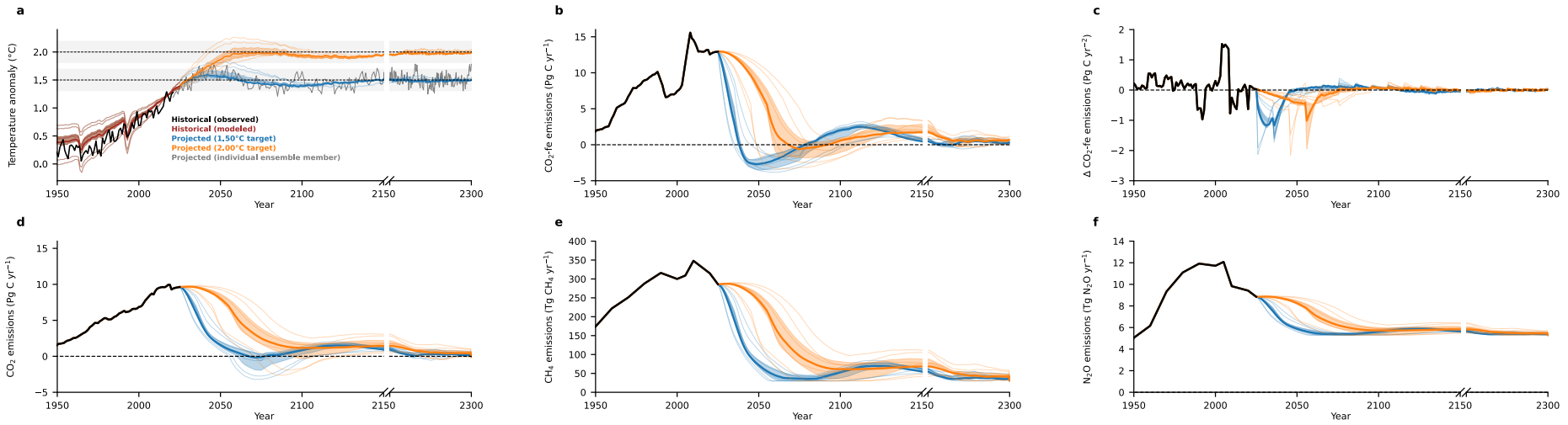

Extended Data Figure 2. Globally averaged surface atmospheric temperature anomaly with respect to 1850-1900, CO_2-fe emissions, their annual rate of change, as well as CO_2, CH_4, and N_2O emissions when applying the adaptive emission reduction approach every ten years. (a) Temperature anomalies with respect to 1850-1900, **(b)** CO_2-fe emissions, and **(c)** their annual rate of change if the AERA is applied every ten years starting in the year 2025 for the 1.5°C target (blue) and the 2.0°C target (orange). In addition, the AERA-calculated emission curves for **(d)** CO_2, **(e)** CH_4, and **(f)** N_2O are shown. As compared to figure 2 in the main text, here the CO_2 emissions are forced to remain constant while only CH_4, N_2O, VOC, NOx, and CO emissions evolve proportionally. The thick solid lines show the average of the 8 simulations with varying magnitude and timing of added inter-annual temperature variability of the Bern3D-LPX model configuration with an ECS of 3.2°C, the thin solid lines show the same for the remaining 8 configurations covering ECS from 1.9 to 5.7°C, and the shaded area shows the range of all configurations that fall within the likely range of ECS as defined by Sherwood et al. (2020)[17]. The grey shading in **(a)** indicates the uncertainty with which the anthropogenic warming can be determined (±0.2°C)[53–56].

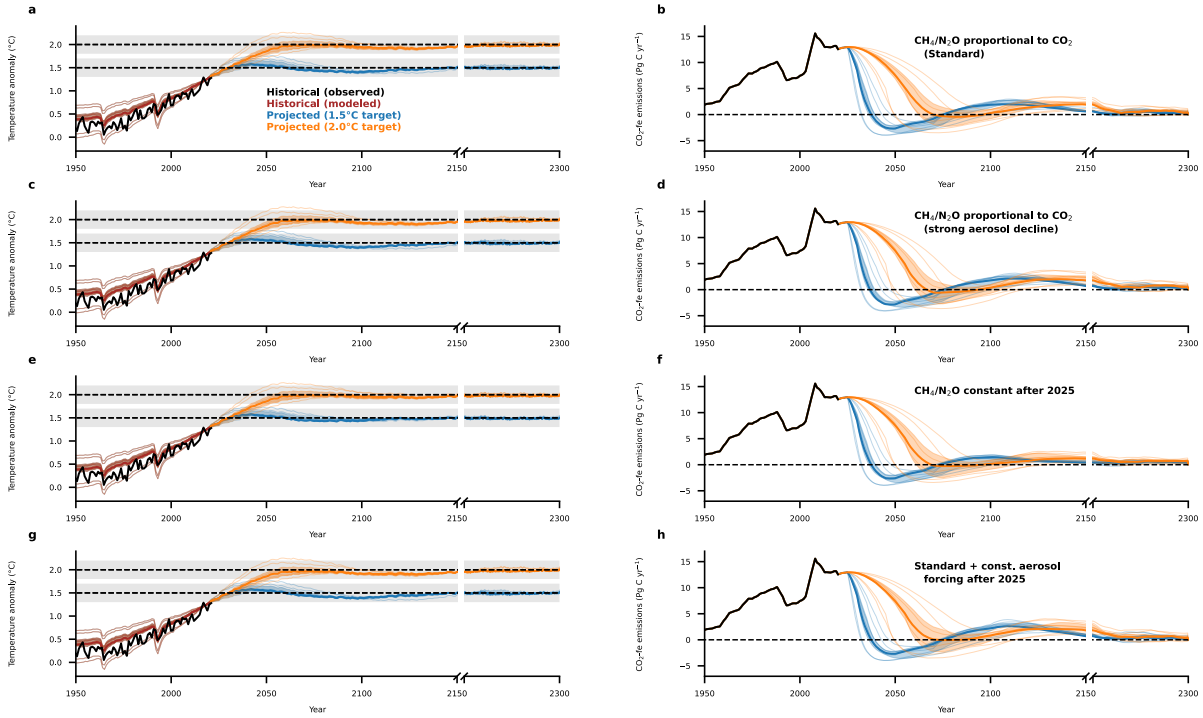

Extended Data Figure 3. Adaptive CO_2-fe emissions and resulting temperature anomaly for 1.5°C and 2.0°C target for different non-CO_2 GHG emissions and aerosol radiative forcing. **(a, c, e, g)** Temperature anomalies with respect to 1850-1900 and **(b, d, f, h)** corresponding CO_2-fe emissions if the AERA is applied every five years starting in the year 2025 for the 1.5°C target (blue) and the 2.0°C target (orange) for four different idealized cases: **(a, b)** aerosol radiative forcing decreases exponentially and CO_2, CH_4, and N_2O emissions evolve proportionally, **(c, d)** aerosol radiative forcing decreases according to the CO_2 emissions and CO_2, CH_4, and N_2O emissions evolve proportionally, **(e, f)** aerosol radiative forcing decreases exponentially but CH_4, and N_2O emissions remain constant after 2025 and only CO_2 evolves dynamically, and **(g, h)** aerosol radiative forcing remains constant after 2025 and CO_2, CH_4, and N_2O emissions evolve proportionally. The thick solid lines show the average of the 8 simulations with varying magnitude and timing of added inter-annual temperature variability of the Bern3D-LPX model configuration with an ECS of 3.2°C and the shaded area shows the range of all configurations that fall within the likely range of ECS as defined by Sherwood et al. (2020)[17]. The grey shading in **(a, c, e, g)** indicates the uncertainty with which the anthropogenic warming can be determined (±0.2°C)[53–56]. The corresponding CO_2, CH_4, and N_2O emissions and aerosol forcing for each simulated case are shown in Figure 3.

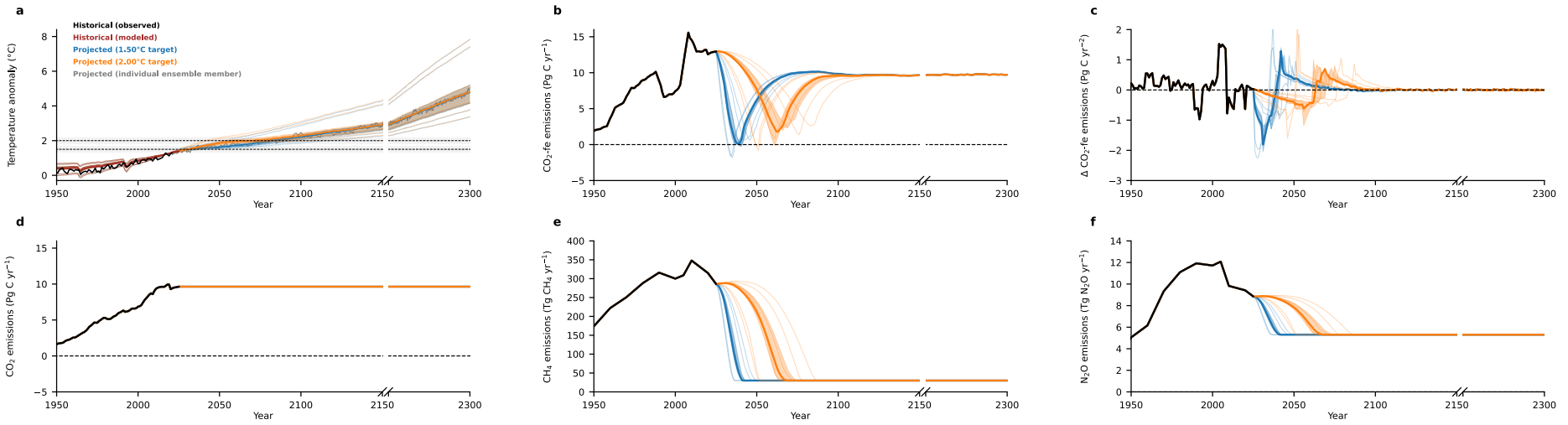

828

829 **Extended Data Figure 4. Globally averaged surface atmospheric temperature anomaly with respect to 1850-1900, CO_2-fe emissions, their annual rate of**
830 **change, as well as CO_2, CH_4, and N_2O emissions following the adaptive emission reduction approach when forcing CO_2 emissions to remain constant. (a)**
831 Temperature anomalies with respect to 1850-1900, **(b)** CO_2-fe emissions, and **(c)** their annual rate of change if the AERA is applied every five years starting in
832 the year 2025 for the 1.5°C target (blue) and the 2.0°C target (orange). In addition, the AERA-calculated emission curves for **(d)** CO_2, **(e)** CH_4, and **(f)** N_2O are
833 shown. As compared to figure 2 in the main text, here the CO_2 emissions are forced to remain constant while only CH_4, N_2O, VOC, NOx, and CO emissions
834 evolve proportionally. The thick solid lines show the average of the 8 simulations with varying magnitude and timing of added inter-annual temperature
835 variability of the Bern3D-LPX model configuration with an ECS of 3.2°C, the thin solid lines show the same for the remaining 8 configurations covering ECS
836 from 1.9 to 5.7°C, and the shaded area shows the range of all configurations that fall within the likely range of ECS as defined by Sherwood et al. (2020)[17]. The
837 grey shading in **(a)** indicates the uncertainty with which the anthropogenic warming can be determined (±0.2°C)[53–56].

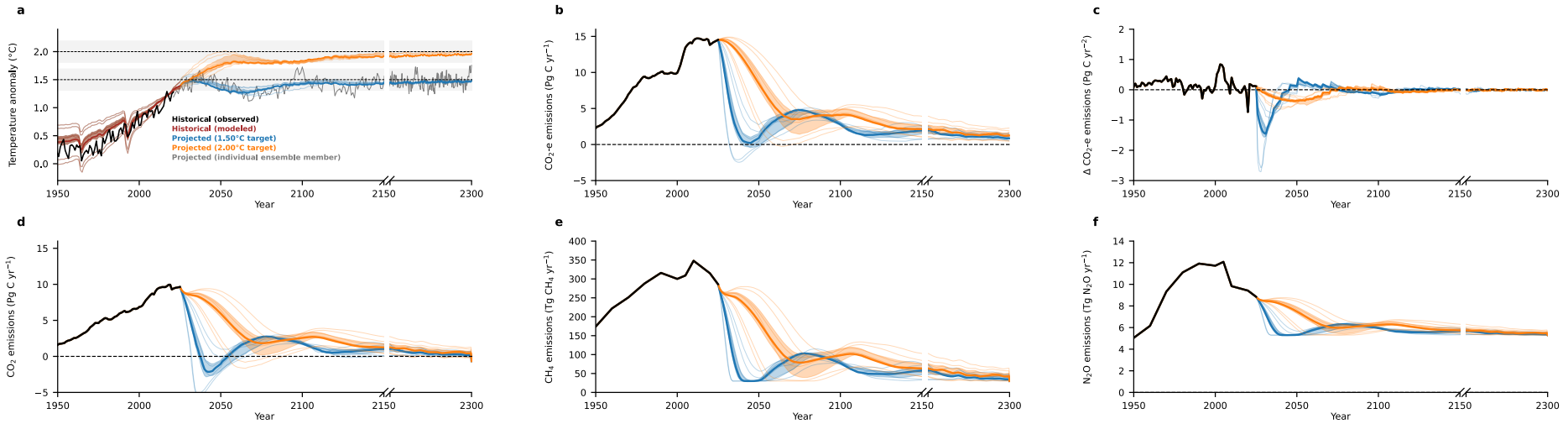

838

839 **Extended Data Figure 5. Globally averaged surface atmospheric temperature anomaly with respect to 1850-1900, CO_2-e emissions, their annual rate of**
840 **change, as well as CO_2, CH_4, and N_2O emissions following the adaptive emission reduction approach using GWP-100 instead of CO_2-fe to split CO_2-e**
841 **emissions. (a)** Temperature anomalies with respect to 1850-1900, **(b)** CO_2-e emissions, and **(c)** their annual rate of change if the AERA is applied every five
842 years starting in the year 2025 for the 1.5°C target (blue) and the 2.0°C target (orange). In addition, the AERA-calculated emission curves for **(d)** CO_2, **(e)** CH_4,
843 and **(f)** N_2O are shown. As compared to figure 2 in the main text, here the GWP-100 approach was used to calculate CO_2 equivalent emissions from CH_4 and
844 N_2O emissions and the CO_2-fe emissions approach was applied to calculate CO_2 equivalent emissions from the remaining forcing agents. The thick solid lines
845 show the average of the 8 simulations with varying magnitude and timing of added inter-annual temperature variability of the Bern3D-LPX model configuration
846 with an ECS of 3.2°C, the thin solid lines show the same for the remaining 8 configurations covering ECS from 1.9 to 5.7°C, and the shaded area shows the
847 range of all configurations that fall within the likely range of ECS as defined by Sherwood et al. (2020)[17]. The grey shading in **(a)** indicates the uncertainty with
848 which the anthropogenic warming can be determined (±0.2°C)[53–56]

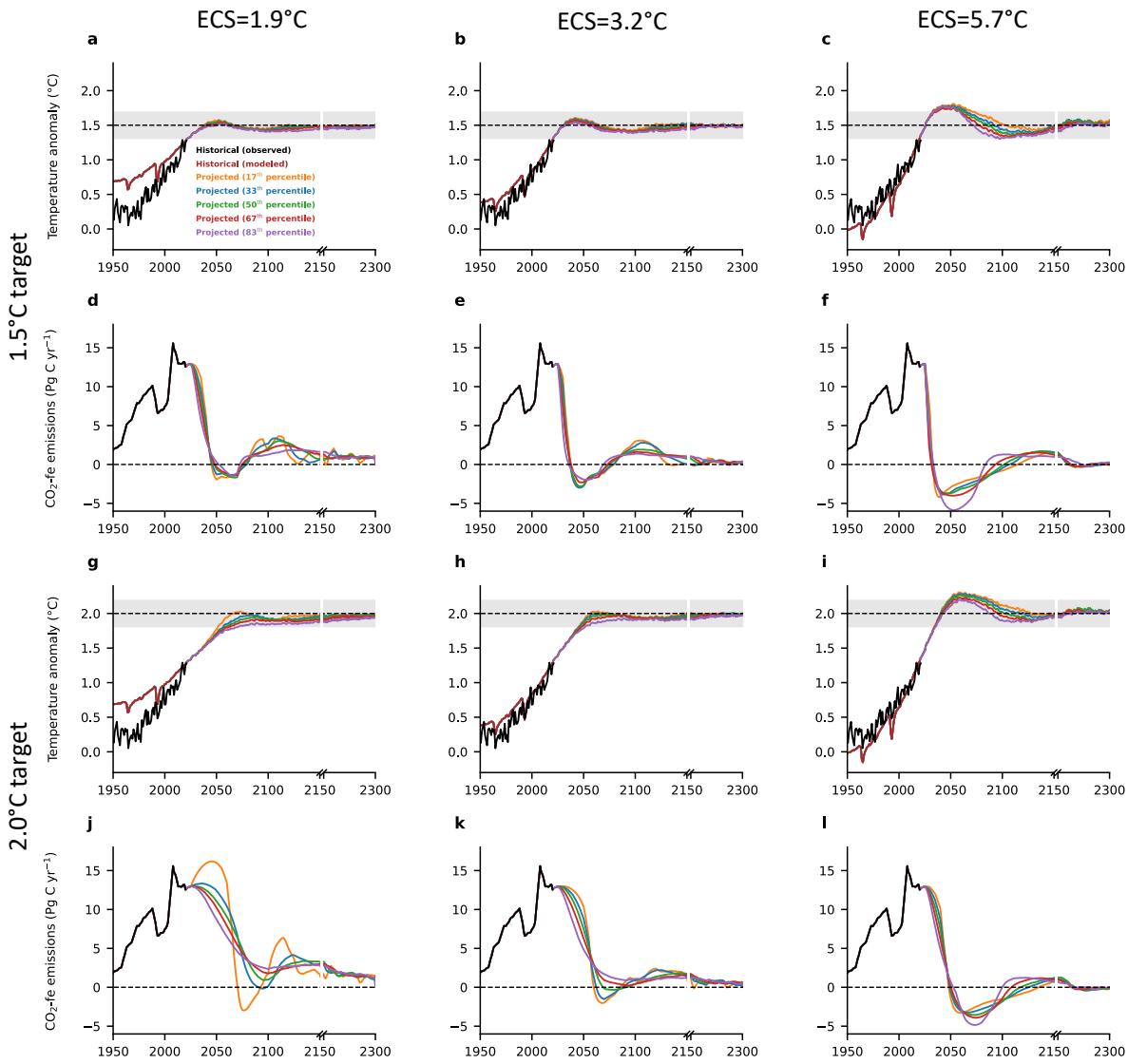

Extended Data Figure 6. Adaptive emissions and resulting temperature anomaly for 1.5°C and 2.0°C target with varying compliance. Temperature from 2020 to 2300 for three model configurations with varying ECS (1.9°C **(a, d, g, j)**, 3.2°C **(b, e, h, k)**, 5.7°C **(c, f, i, l)**) averaged over four simulations each with different inter-annual variability for the **(a-c)** 1.5°C and **(g-i)** 2.0°C temperature target and **(d-f, j-l)** the respective CO_2-fe emission curves with different compliance, i.e., at each stocktake the 17th (orange), 33rd (blue), 50th (green), 67th (red), or 83rd percentile (violet) was implemented. The percentiles are scaled at each stocktake based on the percentiles of the REB in 2020 from Table 5.8 of the IPCC AR6 WG1 report[89]. The grey shading in **(a, b, c, g, h, i)** indicates the uncertainty with which the anthropogenic warming can be determined (±0.2°C)[53–56].

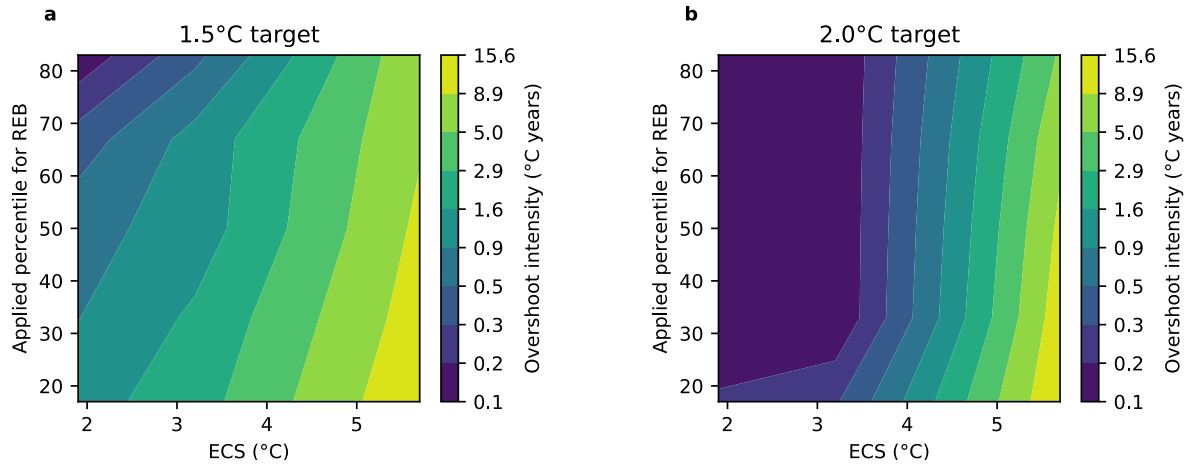

860

861 **Extended Data Figure 7. Overshoot cumulative intensity for 1.5°C and 2°C temperature targets**
862 **dependent on compliance and model configuration.** Overshoot cumulative intensity (°C years), defined
863 as the sum of the overshoot temperatures in each year, in dependence of model configuration (ECS from
864 1.9°C to 5.7°C) and the REB that was used in the AERA (17^{th}, 33^{rd}, 50^{th}, 67^{th}, and 83^{rd} percentile) for **(a)**
865 1.5°C and **(b)** 2°C target.

Supplementary Information

Testing the AERA with Bern3D-LPX

The AERA was tested using the Bern3D-LPX model, version 2.0[62,63] with nine model configurations with combinations of three ocean diapycnal mixing coefficients ($1e^{-4}$, $2e^{-5}$, $1e^{-5}$ m^2 s^{-1}) and three temperature sensitivities to radiative forcing. These three sensitivities to radiative forcing are created by varying an internal Bern3D model parameter that accounts for climate feedbacks, which are not explicitly represented in the model (-0.7, -0.3, 0.1 W m^{-2} K^{-1}). These nine configurations cover the ECS range from 1.9 to 5.7 °C and the TCR range from 1.3 to 2.5 °C. This range represents the range of TCR/ECS estimates based on multiple lines of evidence[24].

For each configuration, the same set of simulations were performed. In these simulations, land-use change CO_2 emissions were interactively simulated by the biosphere component of the Bern3D-LPX model[63] by prescribing land-use area. More specifically, over the historical 1750-2014 period, historical land-use area was prescribed[91]. From 2015 to 2100, land-use area was assumed to follow the low-emissions pathway SSP1-2.6, and from 2100 to 2300 land-use area was assumed to be constant. The corresponding land-use change CO_2 emissions were diagnosed by the difference in air-land CO_2 flux between a simulation with constant land-use area and one with changing land use as prescribed above. Both simulations had the same atmospheric CO_2 concentrations, following historical records until 2014 and SSP1-2.6 afterward[81]. Historical non-CO_2 radiative forcing from 1850 to 2004 was prescribed by values from the RCP database (**https://tntcat.iiasa.ac.at/RcpDb/dsd?Action=htmlpage&page=welcome**)[83–90,92], and non-CO_2 radiative forcing from 2005 to 2025 follows the SSP1-2.6 scenario as described in the SSP database (**https://tntcat.iiasa.ac.at/SspDb/dsd?Action=htmlpage&page=10**)[93,94]. After 2025, the non-CO_2 radiative forcing was either develop dynamically depending on the AERA-prescribed CO_2-fe emissions or was prescribed as a time-series. Before 1850, the non-CO_2 radiative forcing is held

constant at the values from 1850. Historical fossil fuel CO_2 emissions are prescribed from 1765 to 2019 based on the Global Carbon Project[33], and in 2020 based on Le Quéré et al. (2021)[95]. Prescribed fossil fuel CO_2 emissions from 2021 to 2025 are assumed to evolve proportionally to the estimated CO_2-fe emissions that were estimated from the Nationally Determined Contributions (NDC) (Climate Action Tracker[65]).

The different ECSs in each configuration lead to a range of $\Delta T_{ant}^{model}(2020)$ of 0.64 to 1.48°C. Due to this difference, ΔT_{ant}^{target} is defined for each configuration so that $\Delta T_{ant}^{target} - \Delta T_{ant}^{model}(2020)$ equals the $\Delta T_{ant}^{target} - \Delta T_{ant}^{obs}(2020)$ calculated from observations. Thus, for each model configuration the remaining warming from 2020 onwards is the same and differences in the emission curves after 2020 result solely from the differences in ocean mixing and temperature sensitivity and not from differences in the already realized model warming. The historical $\Delta T_{ant}(2020)$ calculated as described above is 1.23°C, leaving an allowable warming of 0.27°C for the 1.5°C target and 0.77°C for the 2°C target.

From 2025 onward, CO_2-fe emissions are calculated by the AERA every 5 years starting in 2025 to mimic the global stocktake process (UNFCCC 2015[6]). For the first step of the AERA, the historical time-series of temperature and RF are needed to calculate the anthropogenic warming at the time of the stocktake. The historical temperature timeseries is directly taken from the simulated model output for each configuration. In addition, an artificial temperature anomaly was added to the simulated temperature in Bern3D, as the modelled inter-annual variability is strongly underestimated. The added anomaly is derived from observed GMST (HadCRUT5) from 1920 to 2019 by subtracting a 3rd order polynomial fit. This 100-year time series is added periodically. To create different anomalies, the anomaly was also added with different phasing (25, 50, and 75 years) and also with a changing sign, resulting in 8 different temperature time series for each model configuration. The past RF is a combination of the CO_2 and non-CO_2. The non-CO_2 RF is directly taken from the prescribed RF to Bern3D-LPX. The CO_2 RF is calculated following IPCC AR6, Table 7.SM.1[96] using the dynamically

simulated atmospheric CO_2 in the respective simulation and prescribed atmospheric N_2O based on the RCP and SSP databases following SSP1-2.6. In the second step, the REB is estimated based on the anthropogenic warming from step one and the past CO_2-fe emission curve. The past CO_2-fe emission curve is the sum of the dynamically adapted fossil fuel CO_2 emissions, the emissions from prescribed land-use area (smoothed with a 21-year running mean due to its relatively large inter-annual variability), and the non-CO_2 forcing agent emissions that are derived from the prescribed non-CO_2 radiative forcing (smoothed with a 5-year running mean to avoid artificially steps in the emissions that arise from the radiative forcing data that is only provided every 10 years). The CO_2 equivalent emissions from non-CO_2 forcing agents are derived from the prescribed non-CO_2 radiative forcing using the CO_2-fe emissions approach[17]. In the last step of the AERA, the REB is distributed over the following years. In the standard case, the CO_2 equivalent emissions are split using the CO_2-fe emissions approach[17]. When testing the AERA with the GWP-100 approach (Extended Data Figure 5), the equivalent CO_2 emissions from CH_4 and N_2O emissions for the period after the stocktake are calculated using GWP-100, while the CO_2-fe emissions approach is used to transfer the radiative forcing from the remaining non-CO_2 forcing agents (aerosols, halogens, …). The effect of CH_4 on tropospheric ozone is accounted for by GWP-100 and only the remaining radiative forcing by ozone, which is mainly caused by CO, VOC, and NOx, and to a small extend by stratospheric ozone, is transferred via the CO_2-fe emissions approach (Supplementary Figure 2).

After the AERA is applied, the future adapted CO_2-fe emission curve is again divided into different components (CO_2 fossil fuel emissions, land use change CO_2 emissions, non-CO_2 emissions). First, the prescribed land-use change CO_2 emissions are subtracted from the CO_2-fe emission curve that was determined from the AERA. The radiative forcing and CO_2-fe emissions from non-CO_2 radiative agents are calculated using a reduced form atmospheric chemistry model[64] updated with the latest information from IPCC AR6. The reduced form atmospheric chemistry model takes time series of CH_4, N_2O, CO, VOC, and NOx emissions, as well as time series of radiative forcing of aerosols and halogens,

as input to calculate future fossil fuel CO_2 emissions and the radiative forcing from non-CO_2 radiative agents from which the corresponding non-CO_2 CO_2-fe emissions are calculated. In the standard case (Figure 2), CO_2, CH_4 and, N_2O emissions after 2025 evolve proportionally and are chosen so that fossil fuel CO_2 emissions and CO_2-fe emissions from non-CO_2 radiative agents fit the prescribed CO_2-fe emissions by the AERA (minus the land use change CO_2 emissions). However, CH_4, and N_2O emissions cannot descend below the thresholds 30 Tg CH_4 yr^{-1} and 5.3 Tg N_2O yr^{-1}, respectively, due to the difficulty in abating CH_4 and N_2O emissions from agricultural and livestock sectors. The N_2O emissions threshold is chosen as the minimum N_2O emissions across the 21st century and across the range of SSPs from the SSP database. The minimum CH_4 emissions prescribed here are below the minimum CH_4 across all SSPs and present the most optimistic future for possible CH_4 reductions. Recent estimates quantify the potential reduction in CH4 emissions until 2030 to be 45-54% (Emissions Gap Report 2021[97] and the Global Methane Initiative (https://www.globalmethane.org/documents/gmi-mitigation-factsheet.pdf)). Here, we assumed that 45% is possible until 2030 and another 45% is possible until 2300. While this is clearly optimistic, large-scale negative CO_2 emissions are also optimistic. In alternative cases (Figure 3 & Extended Data Figure 3), CH_4 and N_2O emissions after 2025 are prescribed and only fossil fuel CO_2 emissions after 2025 are dynamically chosen so that fossil fuel CO_2 emissions and CO_2-fe emissions from non-CO_2 radiative agents fit the prescribed CO_2-fe emissions by the AERA (minus the land use change CO_2 emissions) (Supplementary Figure 2).

Reduced form atmospheric chemistry model

The reduced form atmospheric chemistry model calculates the effective radiative forcing for non-CO_2 radiative forcing agents based on prescribed emissions, as well as time series of radiative forcing of aerosols and halogens[64] with updated equations and constants. The reduced chemistry model is initialized in 2019 from observational data and evolves over time as follows:

- Anthropogenic CH_4 and, N_2O emissions are prescribed as input.

- Natural CH_4 and, N_2O emissions are supposed to be constant over time and are set to 218 Tg CH_4 yr^{-1} and 9.7 Tg N yr^{-1}, respectively. Natural N_2O emissions are taken from Tian et al. (2020)[36] and natural CH_4 emissions are calculated from the change in atmospheric CH_4 mixing ratio from 2000 to 2017 from NOAA (https://gml.noaa.gov/ccgg/trends_ch4/), anthropogenic CH_4 emissions from 2000 to 2017 from the Global Methane Budget[31], and an atmospheric lifetime CH_4 of 9.1 years (based on Tab 6.2 IPCC AR6 and associated text)[98].
- CO, VOC, and NO_X emissions in 2019 are initialized based on the respective emissions in 2020 in the SSP database following SSP1-2.6 (763.5 Tg CO yr^{-1}; 128.6 Tg VOC yr^{-1}; 123.6 Tg NO_2 yr^{-1}). After 2019, these CO, VOC, and NO_X emissions are assumed for simplicity to evolve proportional to CO_2 emissions, although these emissions are linked to a range of sources such as fossil fuel burning, N-fertilizer use, or biomass burning and their relationship with CO_2 emissions may change through time. These emissions are assumed to not be able to drop below their respective emissions in 2100 following SSP1-2.6: 307.2 Tg CO yr^{-1}; 38.4 Tg VOC yr^{-1}; 32.4 Tg NO_2 yr^{-1}.
- Preindustrial and 2019 atmospheric mole fractions of CH_4 (731.41 and 1825.00 ppb) and N_2O (273.87 and 330.50 ppb) are prescribed based on tables 7.5 and 7.SM.1 and chapter 7 of IPCC AR6[96]. After 2019, atmospheric mole fractions of CH_4 and N_2O evolve dynamically as explained below.
- CH_4 mole fraction is calculated forward every year as follows:

$$CH_4(t+1) = CH_4(t) + \frac{ppb}{2.75\ Tg\ CH_4}\left(E_{nat}^{CH_4}(t+1) + E_{ant}^{CH_4}(t+1)\right) - \frac{CH_4(t)}{\tau_{CH_4}(t)},$$

(10)

with $CH_4(t)$ being the CH_4 mole fraction (ppb) in year t, $E_{nat}^{CH_4}$ being the natural CH_4 emissions (Tg CH_4), $E_{ant}^{CH_4}$ being the anthropogenic CH_4 emissions (Tg CH_4), $\frac{ppb}{2.75\ Tg\ CH_4}$ being the conversion

factor from the IPCC AR6 report [99], and $\tau_{CH_4}(t)$ being the life time of CH_4 (yr) that is calculated as follows:

$$\tau_{CH_4}(t) = \left(\frac{rOH}{11yr} + \frac{1}{52.4\ yr}\right)^{-1},$$

(11)

with lifetimes based on Tab 6.2 in IPCC AR6 Chapter 6[96] and Prather et al. (2012)[100] and rOH being the relative change in tropospheric OH with respect to year 2019:

$$\ln(rOH) = ln\left(\frac{OH(t)}{OH(2019)}\right) =$$

$$-0.32 * \ln\left(\frac{CH_4(t)}{CH_4(2019)}\right) + 0.0042 * \left(\frac{E_{NO_X}(t)}{E_{NO_X}(2019)}\right) - 0.000105 * \left(\frac{E_{CO}(t)}{E_{CO}(2019)}\right) - 0.000313 * \left(\frac{E_{VOC}(t)}{E_{VOC}(2019)}\right), \text{(12)}$$

with $E_{NO_X}(t)$, $E_{CO}(t)$, and $E_{VOC}(t)$ being the emissions from CO, VOC, and NO_X.

- N_2O concentrations change is calculated forward every year as follows:

$$N_2O(t+1) = N_2O(t) + \frac{ppb}{4.79\ Tg\ N}\left(E_{nat}^{N_2O}(t+1) + E_{ant}^{N_2O}(t+1)\right) - \frac{N_2O(t)}{\tau_{N_2O}(t)}yr,$$

(13)

with $N_2O(t)$ being the N_2O concentrations (ppb) in year t, $E_{nat}^{N_2O}$ being the natural N_2O emissions (Tg N), $E_{ant}^{N_2O}$ being the anthropogenic N_2O emissions (Tg N), $\frac{ppb}{4.79\ Tg\ N}$ being the conversion factor from Prather et al. (2012)[100], and $\tau_{N_2O}(t)$ being the lifetime of N_2O (yr)[64]:

$$\tau_{N_2O}(t) = 116\ yr * \left(\frac{E_{ant}^{N_2O}(t)}{E_{ant}^{N_2O}(2019)}\right)^{-0.055},$$

(14)

with the mean lifetime (116 years) being based on chapter 5 of IPCC AR6[99].

- The stratospheric adjusted radiative forcing for CH_4 and N_2O is calculated as described in chapter 7 of IPCC AR6, Table 7.SM.1[96]. From that, the effective radiative forcing is calculated using adjustment factors (0.86 for CH_4 and 1.07 for N_2O) from chapter 7 of IPCC AR6[96].
- Effective radiative forcing of tropospheric O_3 in 2019 is set to 0.34 W m^{-2} and evolves over time as described in equation 7.SM.1.3 in IPCC AR6 CH7[96]. The effective radiative forcing of tropospheric O_3 in 2019 is within the uncertainty range given in Figure 7.6 in IPCC AR6 CH7[96]. Although the best estimate is 0.47 W m^{-2}, we have reduced the effective radiative forcing so that the total non-CO_2 radiative forcing in 2025 that is estimated by the reduced atmospheric chemistry model is consistent with the prescribed non-CO_2 radiative forcing in Bern3D based on the RCP and SSP databases following SSP1-2.6 that was used until 2025. The effective radiative forcing of stratospheric O3 is of the order of -0.05 W m^{-2} and included in the remaining effective radiative forcing (see below).
- Total halogen effective forcing radiative forcing in 2019 is set to 0.41 W m^{-2} (Figure 7.6 in IPCC AR6 CH7[96]) is divided into short-lived halogens with a lifetime of 12 years (0.08 W m^{-2}), medium-lived halogens with a lifetime of 40 years (0.09 W m^{-2}), long-lived halogens with a lifetime of 100 years (0.21 W m^{-2}), and 'eternal' halogens (0.03 W m^{-2}) based on table 7.SM.1.3 in IPCC AR6 CH7[96]. The halogen radiative forcing is assumed to decay depending on the lifetime with no source of halogens.
- The aerosol effective radiative forcing is set to -1.1 W m^{-2} in 2019 following Figure 7.6 in IPCC AR6 Chapter 7[96]. After 2019, the aerosol forcing decays exponentially in the standard case. Half of it is assumed to decline with a half-life of 20 years and half is assumed to decay with a half-life of 250 years to approximate an aerosol forcing that co-evolves with the strong reductions in CO_2 emissions that need to be achieved to limit warming to temperatures between 1.5°C and 2°C.

- Effective radiative forcing of stratospheric water vapor ($ERF_{H_2O}(t)$) is calculated based on the atmospheric CH_4 mixing ratio in the respective year ($CH_4(t)$) and the preindustrial atmospheric CH_4 mixing ratio (CH_4^{pi})[64]:

$$ERF_{H_2O}(t) = \alpha_{H_2O}\left(\sqrt{CH_4(t)} - \sqrt{CH_4^{pi}}\right), \quad (15)$$

With α_{H_2O} set to 0.0031 $\frac{W}{m^2\ ppb^{\frac{1}{2}}}$ so that $ERF_{H_2O}(2019)$ is 0.05 $\frac{W}{m^2}$ as in Figure 7.6 in IPCC AR6 Chapter 7[96].

- Remaining effective radiative forcing (albedo, stratospheric O_3, contrails, …) is for simplicity assumed to stay constant at -0.07 W m^{-2} based on Figure 7.6 in IPCC AR6 CH7[96].

AERA robustness tests

The AERA was tested for robustness within the Bern3D-LPX model framework. These tests are made with the standard version (CO_2-fe approach and CO_2, CH_4, and N_2O emissions evolving proportional after 2025) and include varying the allowed difference to the REB (ξ) and the allowed integrated exceedance emissions (ε) when fitting the future total CO_2-fe emissions curve, and testing the algorithm when Bern3D has been used with different non-CO_2 GHG radiative forcing than that 'seen' by the AERA to ensure that the AERA still works even if the past radiative forcing estimates are incorrect.

The sensitivities towards the allowed difference to the REB (ξ) and the allowed exceedance emissions (ε) were tested with three model configurations (ECS=1.9°C, 3.2°C, 5.7°C) with 4 instead of 8 different temperature anomalies superimposed in each case for computational reasons. Simulations were made

with half and twice the amount of ξ and ε. CO_2-fe emissions from 2025 to 2300 are on average not different from the standard version when ξ is halved or doubled (0.0 ± 0.1 Pg C yr^{-1}), but minimum CO_2-fe emissions in the 21st century are marginally less pronounced if ξ is halved and more pronounced if ξ is doubled (Supplementary Figure 3). The temperature curves are also indifferent. When exceedance emissions are halved, temperature curves remain almost unchanged, whereas CO_2-fe emissions become less smooth when the temperature anomaly is close to the temperature target (Supplementary Figure 4). In such a situation, a fast change in the sign of the REB between two stocktakes due to natural variability in the temperature likely causes the abrupt changes in the CO_2-fe emissions curve. When ε is doubled, the temperature overshoot in the 21st century becomes larger for the high ECS configuration by up to 0.06°C but leaves temperature curves for the other configurations unchanged. In return, the CO_2-fe emissions curves become slightly smoother. Overall, the chosen best parameters for ξ and ε present the best compromise between the smoothness of the emission curves and the degree of a temperature overshoot.

To test the robustness of the AERA towards the estimate of the past radiative forcing, the radiative forcing from aerosols was adjusted in the model, whereas the non-CO_2 radiative forcing and the corresponding CO_2-fe that are 'seen' by the AERA are not adjusted. The radiative forcing of aerosols in 2011 was taken from the central estimate of the IPCC report WG1 2013[59]. It was extrapolated back and forward (until 2025) in time using sulfur emissions as a proxy from the RCP and SSP databases. After 2025, the radiative forcing is calculated by the reduced form chemistry model. Once the aerosol radiative forcing time series is determined, this timeseries of aerosol forcing was adjusted by ±40%. The model was then run with 3 different configurations (ECS =1.9, 3.2 and 5.7°C). However, only a few combinations of ECS and adjusted aerosol forcing are credible, i.e., a small aerosol forcing in combination with a large ECS results in too strong warming over the historical period whereas a small ECS and a large cooling aerosol forcing results in almost no temperature rise over the same period. We then chose the combinations that represent the historical warming best: low ECS and low aerosol

forcing and high ECS and high aerosol forcing (Supplementary Figure 5). Overall, the AERA still works in both cases. If aerosol forcing is less strong than expected, a reduction of aerosols does not cause the expected warming and emissions reductions can be less pronounced. However, if aerosol forcing is underestimated, a reduction of aerosols over the 21st century will cause pronounced warming and an overshoot of 0.58°C to which the AERA reacts with strong emissions reductions. The AERA thus automatically corrects the underestimation of the aerosol forcing.

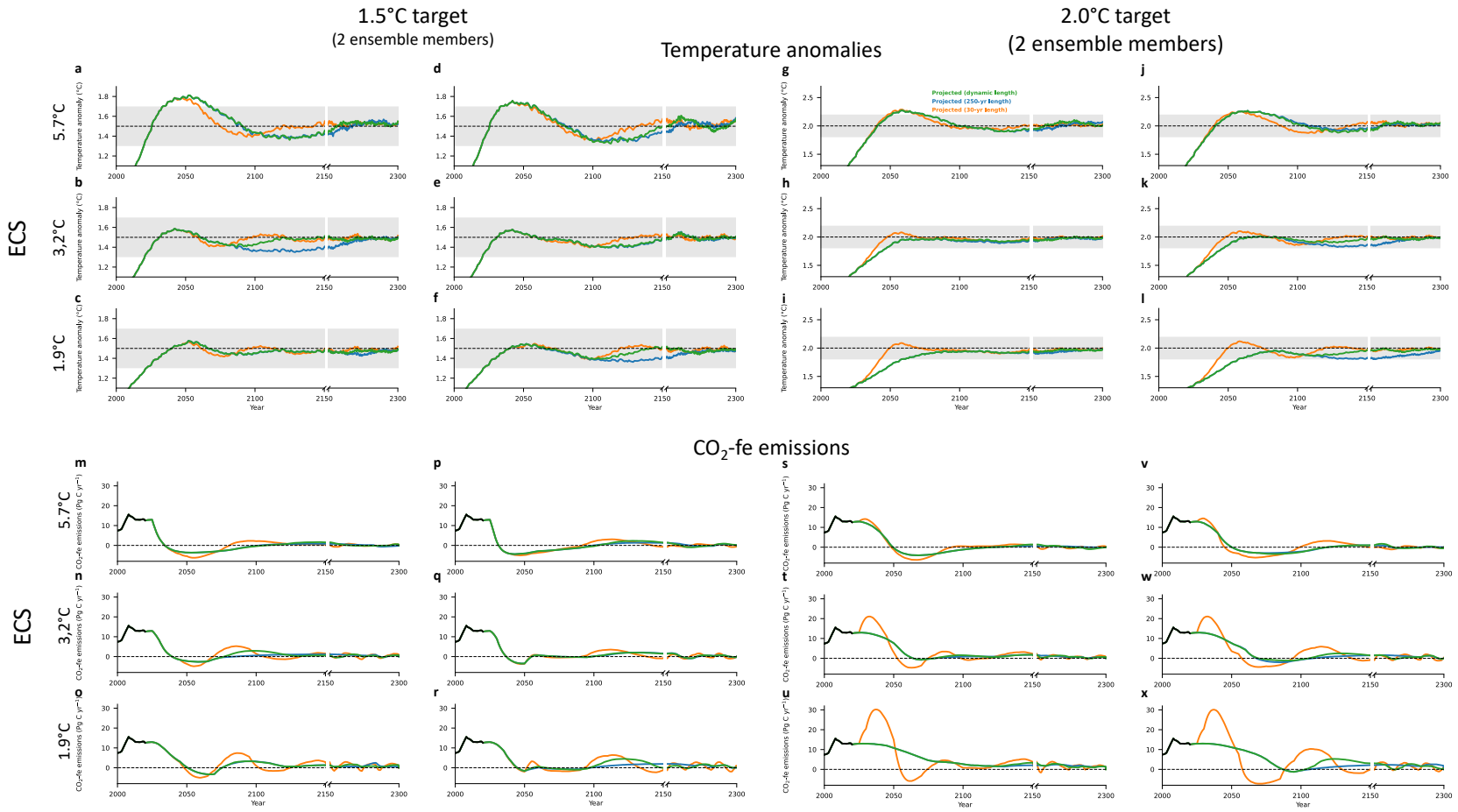

Supplementary Figure 1. Sensitivity of results to maximum length of the prescribed polynomic function in the AERA algorithm. (a-l) Temperature anomalies with respect to 1850-1900 and **(m-x)** corresponding CO_2-fe emissions for two ensemble members each if the AERA is applied every five years starting in the

year 2025 for the 1.5°C target **(a-f, m-r)** and the 2.0°C target **(g-l, s-x)**. The lines show realizations for different maximum lengths of the prescribed polynomic function in the AERA algorithm: fixed maximum length at 30 years (orange), fixed maximum length at 250 years (blue), and dynamical maximum length (green) as described in the methods. The shaded area shows the range of all configurations that fall within the likely range of ECS as defined by Sherwood et al. (2020)[17]. The grey shading in **(a)** indicates the uncertainty with which the anthropogenic warming can be determined (±0.2°C)[53–56].

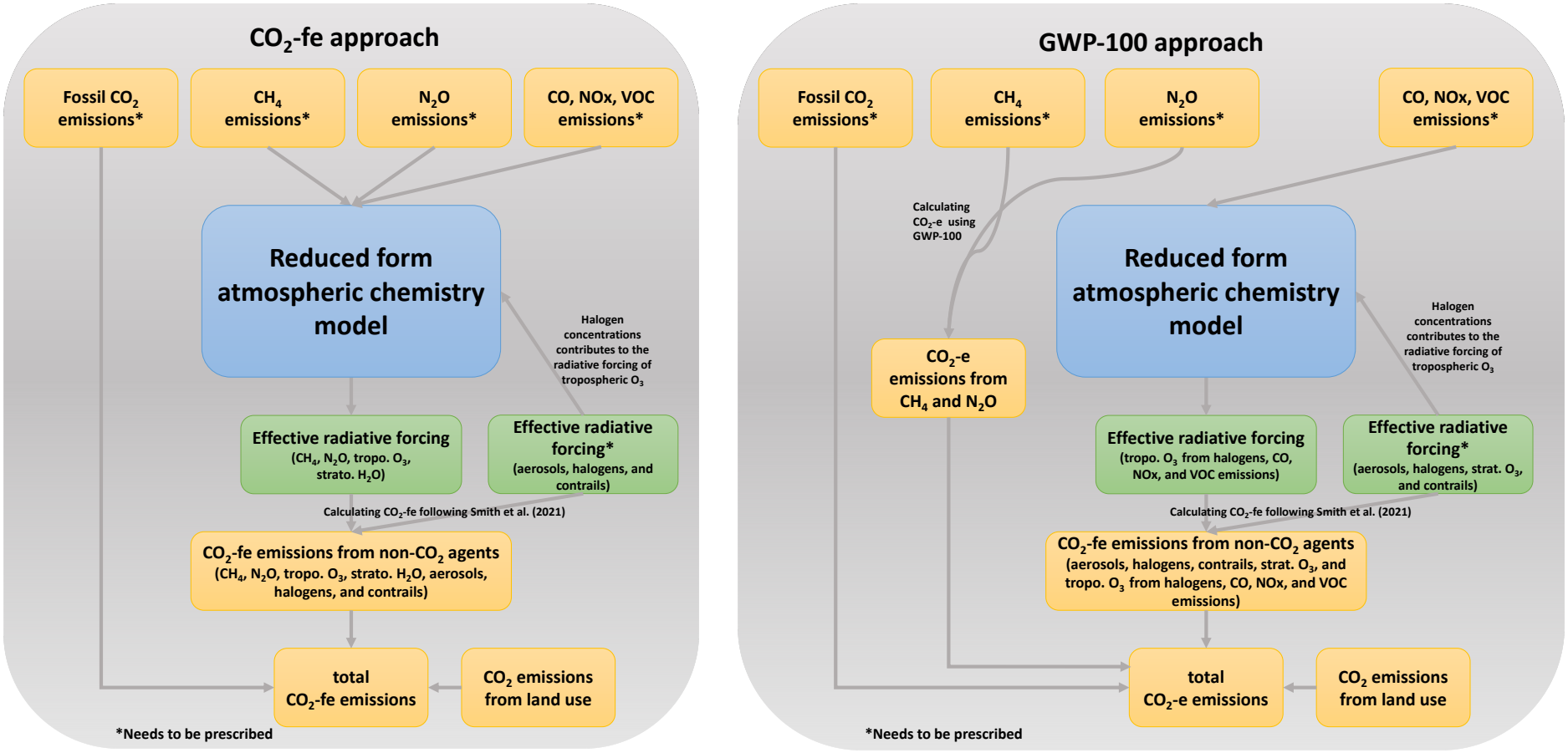

Supplementary Figure 2. Schematic of the implementation of the reduced atmospheric chemistry model. The reduced form atmospheric chemistry model is used to project non-CO_2 GHG concentrations and non-CO_2 (effective) radiative forcing from emissions of CO_2, CH_4, and N_2O, and of the precursors CO, VOC, and NOx. Here, radiative forcing from aerosols and from halogens is prescribed (see methods). When using the CO_2-fe approach to calculate CO_2 equivalent emissions (left), radiative forcing from all non-CO_2 agents considered is added to yield total non-CO_2 radiative forcing, which is converted to CO_2-fe emissions (Smith et al., 2021). When using the GWP-100 approach to calculate CO_2 equivalent emissions (right), CH_4 and N_2O emissions are transferred to CO_2 equivalent

emissions using GWP-100, while radiative forcing from all remaining non-CO_2 agents considered is added to yield the remaining non-CO_2 radiative forcing, which is converted to CO_2-fe emissions. Projected non-CO_2 radiative forcing (together with fossil CO_2 emissions, and land use) is prescribed to the Bern3D-LPX model to project CO_2 concentration and global warming. In the standard simulations in this manuscript, the CH_4, N_2O, CO, NOx, and VOC emissions evolve proportional to the CO_2 emissions in every year and the effective radiative forcing of aerosols and halogens are prescribed. In each year, the CO_2 emissions are chosen for which the resulting CO_2-fe emissions fit the prescribed CO_2-fe emissions by the AERA for that respective year.

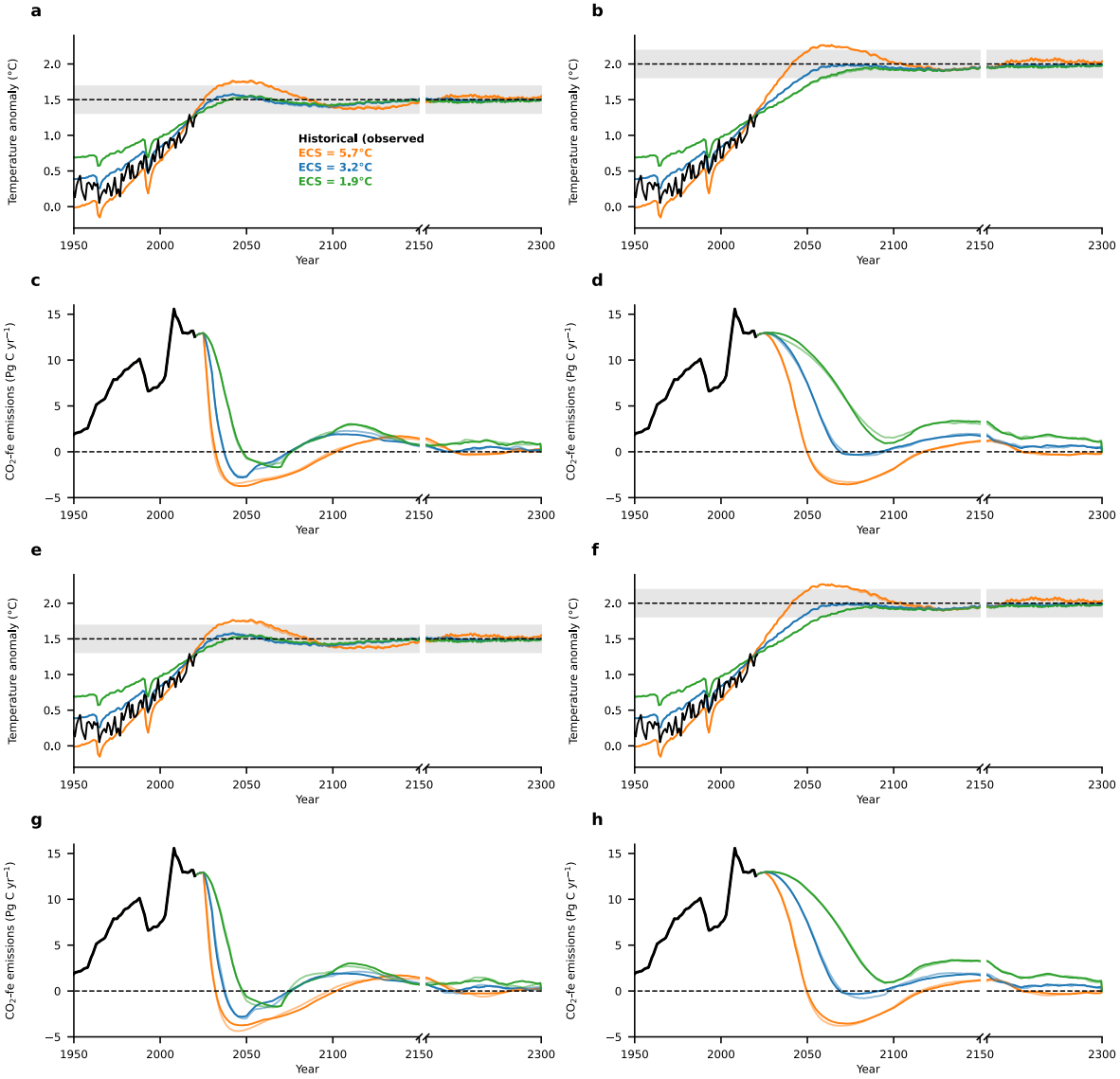

Supplementary Figure 3. Adaptive emissions and resulting temperature anomaly for 1.5°C and 2.0°C target with varying allowed difference to the remaining emission budget. Temperature from 2020 to 2300 for three model configurations with varying ECS (orange = 5.7°C, blue = 3.2°C, and green = 1.9°C) averaged over four simulations each with different inter-annual variability for the **(a, e)** 1.5°C and **(b, f)** 2.0°C temperature target and **(c, d, g, h)** the respective CO_2-fe emission curves with the difference to the remaining emission budget (ξ) being **(a-d)** 2.5 Pg C (half of standard version) and **(e-h)** 10 Pg C. Temperature and emission curves are also shown for the standard version (ξ = 5 Pg C) (colored transparent lines). The grey shading in **(a, b, e, i)** indicates the uncertainty with which the anthropogenic warming can be determined (±0.2°C)[53–56]**.**

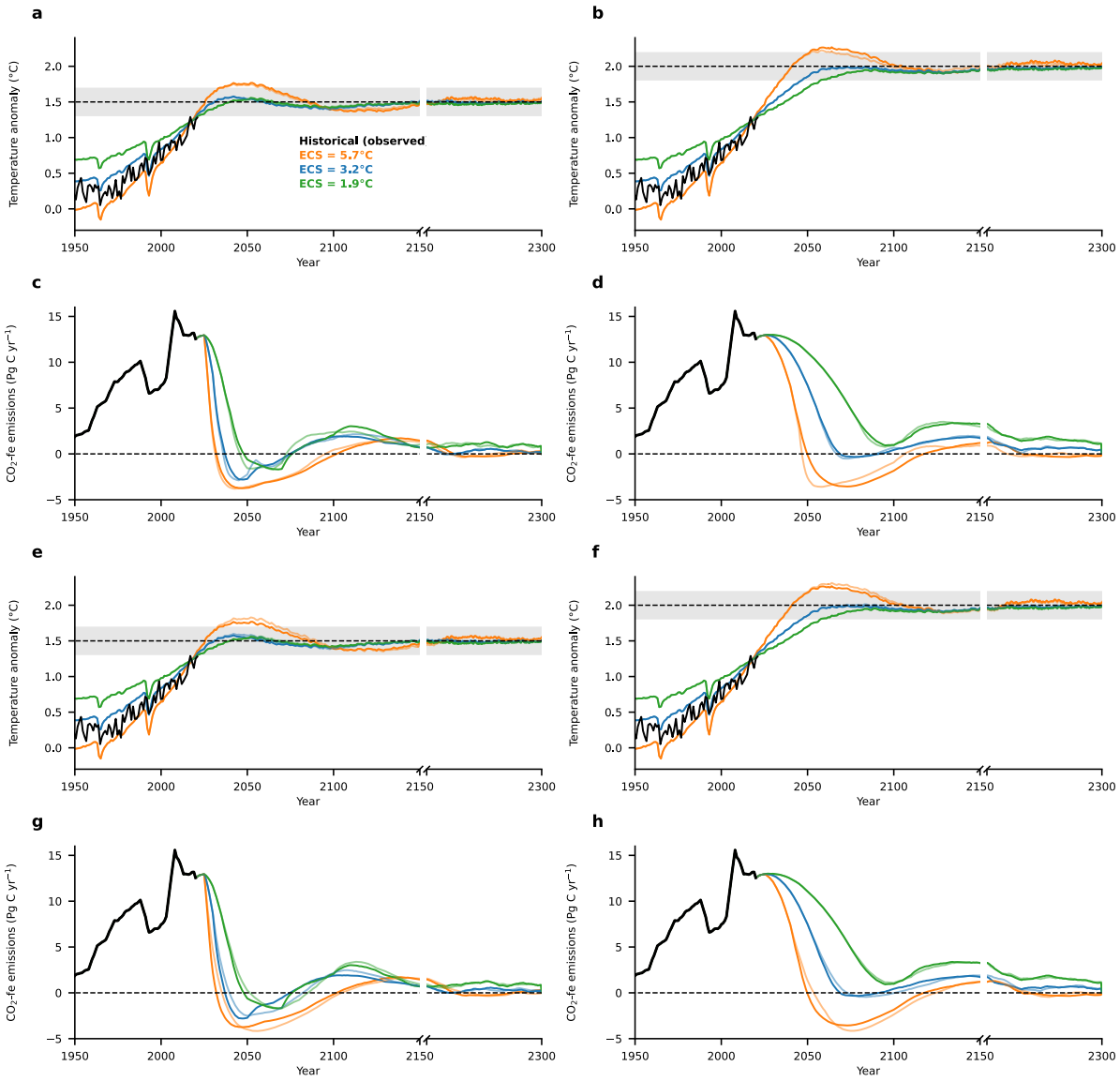

Supplementary Figure 4. Adaptive emissions and resulting temperature anomaly for 1.5°C and 2.0°C target with varying allowed exceedance emissions. Temperature from 2020 to 2300 for three model configurations with varying ECS (orange = 5.7°C, blue = 3.2°C, and green =1.9°C) averaged over four simulations each with different inter-annual variability for the **(a, e)** 1.5°C and **(b, f)** 2.0°C temperature target and **(c, d, g, h)** the respective CO_2-fe emission curves with the allowed exceedance emissions (ε) being **(a-d)** 5 Pg C (half of standard version) and **(e-h)** 20 Pg C. Temperature and emission curves are also shown for the standard version (ε = 10 Pg C) (colored transparent lines). The grey shading in **(a, b, e, i)** indicates the uncertainty with which the anthropogenic warming can be determined (±0.2°C)[53–56].

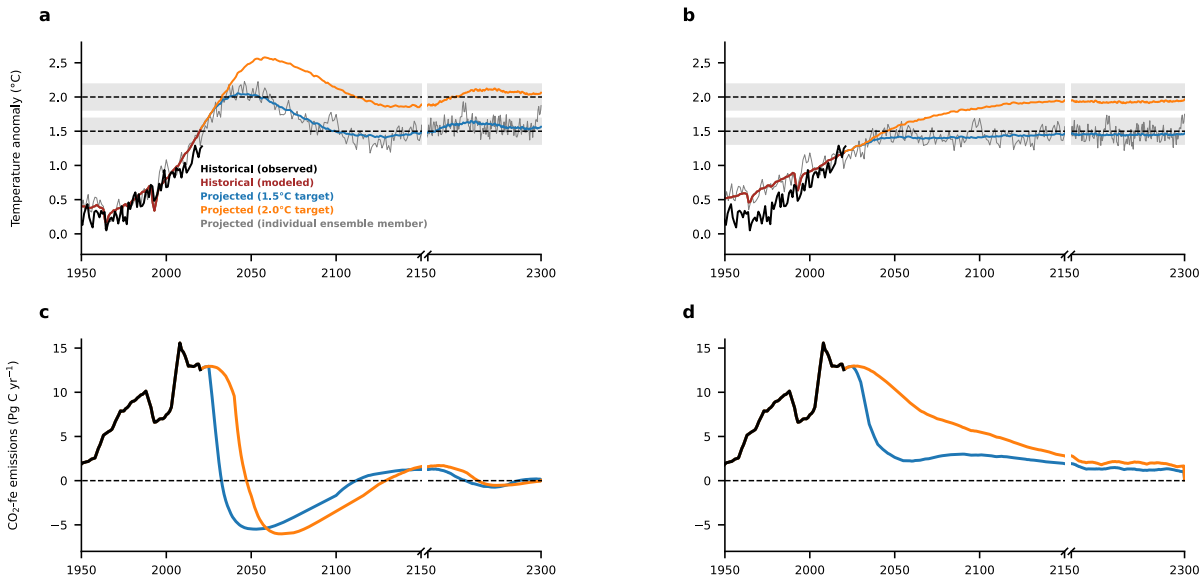

Supplementary Figure 5. Adaptive emissions and resulting temperature anomaly for 1.5°C and 2.0°C target when the radiative forcing from aerosols is different than estimated. (a, b) temperatures and **(c, d)** associated CO_2-fe emissions averaged over four simulations each with different inter-annual variability **(a, c)** with ECS=5.7 and 40% increased simulated radiative forcing from aerosols and **(b, d)** with ECS=1.9 and 40% reduced simulated radiative forcing from aerosols. In each case, the AERA input for the radiative forcing from aerosols was not changed. Temperature observations based HadCRUT5 GMST time series are shown in comparison for the historical period.

References – Supplementary Information

91. Hurtt, G. C. *et al.* Harmonization of global land use change and management for the period 850–2100 (LUH2) for CMIP6. *Geosci Model Dev* **13**, 5425–5464 (2020).
92. van der Werf, G. R. *et al.* Interannual variability in global biomass burning emissions from 1997 to 2004. *Atmos Chem Phys* **6**, 3423–3441 (2006).
93. Riahi, K. *et al.* The Shared Socioeconomic Pathways and their energy, land use, and greenhouse gas emissions implications: An overview. *Global Environmental Change* **42**, 153–168 (2017).
94. van Vuuren, D. P. *et al.* Energy, land-use and greenhouse gas emissions trajectories under a green growth paradigm. *Global Environmental Change* **42**, 237–250 (2017).
95. le Quéré, C. *et al.* Fossil CO2 emissions in the post-COVID-19 era. *Nat Clim Chang* **11**, 197–199 (2021).
96. Forster, P. *et al.* The Earth's Energy Budget, Climate Feedbacks, and Climate Sensitivity. *Climate Change 2021: The Physical Science Basis. Contribution of Working Group I to the Sixth Assessment Report of the Intergovernmental Panel on Climate Change* Preprint at (2021).
97. Drew Shindell *et al.* The role of anthropogenic methane emissions in bridging the emissions gap. in *Emissions Gap Report 2021: The Heat Is On* (2021).
98. Naik, V. *et al.* Short-Lived Climate Forcers. *Climate Change 2021: The Physical Science Basis. Contribution of Working Group I to the Sixth Assessment Report of the Intergovernmental Panel on Climate Change* Preprint at (2021).
99. Canadell, J. G. *et al.* Global Carbon and other Biogeochemical Cycles and Feedbacks. *Climate Change 2021: The Physical Science Basis. Contribution of Working Group I to the Sixth Assessment Report of the Intergovernmental Panel on Climate Change* Preprint at (2021).
100. Prather, M. J., Holmes, C. D. & Hsu, J. Reactive greenhouse gas scenarios: Systematic exploration of uncertainties and the role of atmospheric chemistry. *Geophys Res Lett* **39**, (2012).